Clemson University
College of Engineering and Science
Control and Robotics (CRB) Technical Report

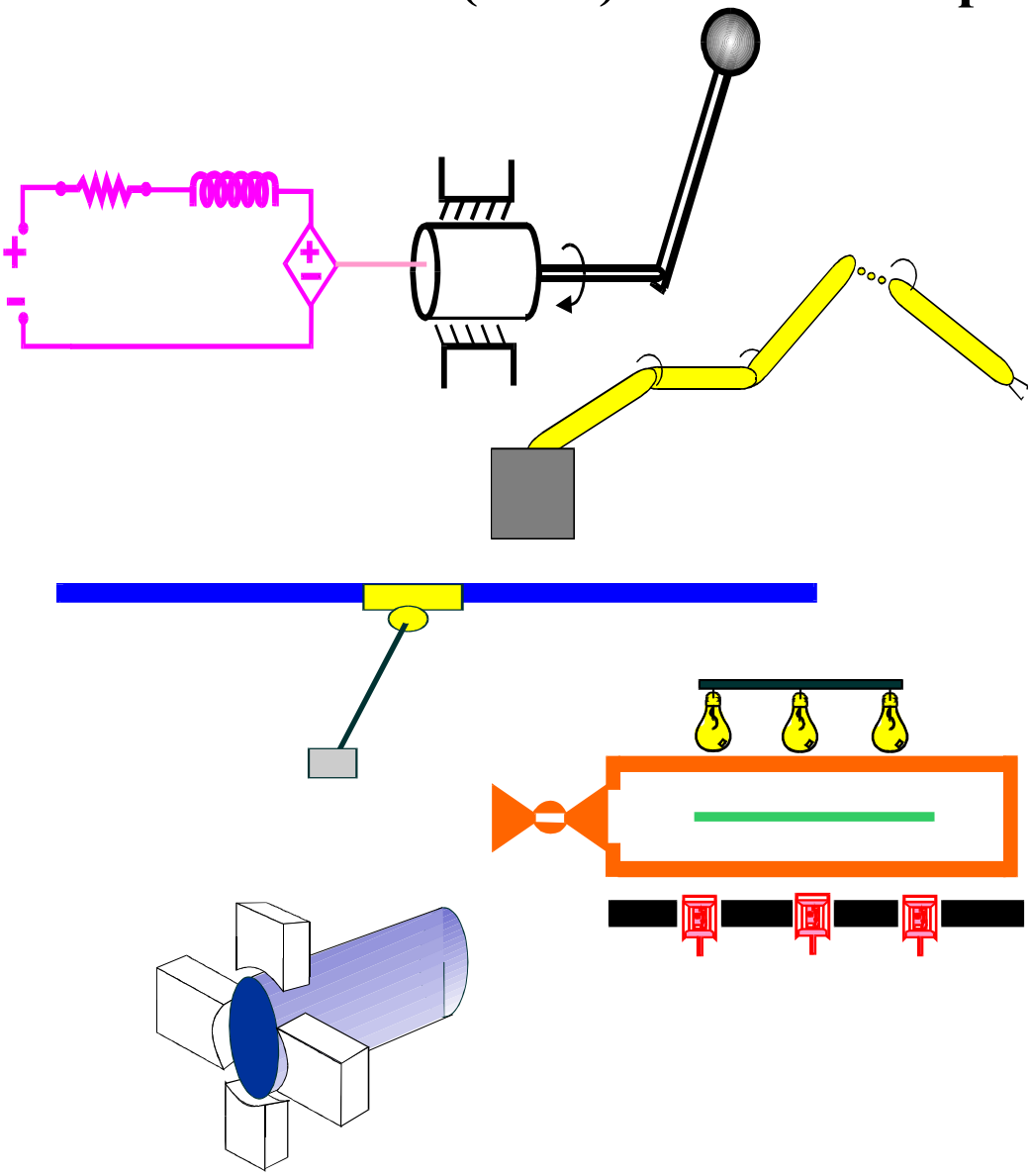

Number: CU/CRB/2/28/06/#1

Title: Coordination Control for Haptic and Teleoperator Systems

Authors: E. Tatlicioglu, M. McIntyre, D. Dawson, and T. Burg

Report Documentation Page

Form Approved
OMB No. 0704-0188

1. REPORT DATE	2. REPORT TYPE	3. DATES COVERED
2006		**00-00-2006 to 00-00-2006**

4. TITLE AND SUBTITLE	5a. CONTRACT NUMBER
Coordination Control for Haptic and Teleoperator Systems	5b. GRANT NUMBER
	5c. PROGRAM ELEMENT NUMBER
6. AUTHOR(S)	5d. PROJECT NUMBER
	5e. TASK NUMBER
	5f. WORK UNIT NUMBER
7. PERFORMING ORGANIZATION NAME(S) AND ADDRESS(ES) **Clemson University,Department of Electrical & Computer Engineering,Clemson,SC,29634-0915**	8. PERFORMING ORGANIZATION REPORT NUMBER
9. SPONSORING/MONITORING AGENCY NAME(S) AND ADDRESS(ES)	10. SPONSOR/MONITOR'S ACRONYM(S)
	11. SPONSOR/MONITOR'S REPORT NUMBER(S)

12. DISTRIBUTION/AVAILABILITY STATEMENT
Approved for public release; distribution unlimited

13. SUPPLEMENTARY NOTES
The original document contains color images.

14. ABSTRACT

15. SUBJECT TERMS

16. SECURITY CLASSIFICATION OF:			17. LIMITATION OF ABSTRACT	18. NUMBER OF PAGES	19a. NAME OF RESPONSIBLE PERSON
a. REPORT	b. ABSTRACT	c. THIS PAGE			
unclassified	**unclassified**	**unclassified**		**22**	

Coordination Control for Haptic and Teleoperator Systems*

E. Tatlicioglu, M. McIntyre, D. Dawson, and T. Burg†

Abstract: In this paper, two controllers are developed for nonlinear haptic and teleoperator systems for coordination of the master and slave systems. The first controller is proven to yield a semi-global asymptotic result in the presence of parametric uncertainty in the master and the slave dynamic models provided the user and the environmental input forces are measurable. The second controller yields a global asymptotic result despite unmeasurable user and environmental input forces provided the dynamic models of the master and slave are known. These controllers rely on a transformation and a flexible target system to allow the master system's impedance to be easily adjusted so that it matches a desired target system. This work also offers a structure to encode a velocity field assist mechanism to provide the user help in controlling the slave system in completing a pre-defined contour following task. For each controller, Lyapunov-based techniques are used to prove that both controllers provide passive coordination of the haptic/teleoperator system when the velocity field assist mechanism is disabled. When the velocity field assist mechanism is enabled, the analysis proves the coordination of the haptic/teleoperator system. Simulation results are presented for both controllers.

1 Introduction

For the purposes of this research, the following definitions are made. A teleoperator system enables a user to execute a remote task with an output system (i.e., a slave system) operating in a physical environment by manipulating an input system (i.e., a joystick or a master system) while providing feedback on the input system. A haptic system is similar to a teleoperator system with the exception that the slave system operates in a virtual environment. Some common application areas for teleoperator and haptic systems include handling hazardous materials, maneuvering mobile robots, underwater vehicles, and microsurgery in either a physical or a virtual environment. The operator's ability to accurately complete these tasks is affected by the transparency of the teleoperator or haptic system. Tactile and force feedback from the system controller along with assistive mechanisms greatly increase the user's performance in completing the desired task [8]. Tactile and force feedback provides the user of the system with a sense of feel or sense of *telepresence* [32] of what the slave system is experiencing in either a physical or a virtual environment. Assistive mechanisms can be integrated into the system controller in various ways. One example, which will be discussed further in subsequent sections of this paper, is the encoding of a tracking objective in the master system that assists the user in completing a pre-defined task (i.e., consider a teleoperator grinding application where the remote user controls the slave system to track a repeated circular path to complete the desired task).

Both the teleoperator and/or haptic problem are theoretically challenging due to issues that impact the user's ability to impart a desired motion on the remote environment while maintaining a sense of feel through the system controller. This problem is further complicated due to the fact that master system apparent inertia is normally very different than that of the slave system that is operating in the remote environment, be it physical or virtual. If the apparent inertia of the master system could be adjusted by the system controller to appear like that of the slave systems, the operator's sense of *telepresence* would be achieved, hence, increasing the user's ability to operate the slave system. To address the above control objective, commercially available haptic systems come in two distinct classes: impedance controlled devices, and admittance controlled devices [35]. Both classes have advantages/disadvantages depending on the application, see [8] and [35] for more details.

The focus of some of the previous teleoperator system research has been to achieve ideal transparency between the environment and the user. In [10], Hannaford modeled the teleoperator system as a two-port network where an estimate of the impedance of the slave system is required to achieve transparency. In [6], *a priori* knowledge of the environmental inputs to the slave system is required to achieve the transparency control objective. Controllers aiming at low-frequency transparency were suggested in [9], [14], and [31]. Frequency-based control designs given in [6], [9], [10], [14], and [31] are for linear teleoperator systems. The concept of the four-channel architecture, which assumes knowledge of system impedances was introduced by the authors of [14] and [37]. To overcome parametric uncertainties, common in teleoperator systems, adaptive controllers were developed in [5], [12], [22], [29], [33], and [38].

Other research has focused on maintaining safe and sta-

*This work is supported in part by two DOC Grants, an ARO Automotive Center Grant, a DOE Contract, a Honda Corporation Grant, and a DARPA Contract.

†The authors are with the Department of Electrical & Computer Engineering, Clemson University, Clemson, SC 29634-0915. E-mail: etatlic@clemson.edu

ble operation of the teleoperator system through passivity concepts. In [1], Anderson and Spong transformed the time delay problem of the teleoperator system into a transmission line problem and presented a controller for the communication circuit that guarantees passivity of the teleoperator system independent of time delay present in the communication block. In [26], Niemeyer and Slotine extended the results in [1], and introduced wave-variables formulation to represent transmission delays, which results in a new configuration for force-reflecting teleoperation. These results were then extended to solve the position tracking problem where [4] and [27] provided a solution when the time delay is constant and [3] provided a solution when the time delay is time-varying. In [17], a passive decomposition for linear dynamically similar systems is introduced. In [15], Lee and Li extended these results to define a nonlinear decomposition which achieves passivity of the master and the slave robots by decomposing the closed-loop teleoperator system into two sub-systems. The reader is referred to [16], [18], and [19] for improvements of passive decomposition. In [20] and [21], Lee suggested a controller for a master and multiple cooperative slave robots over a communication network in the presence of a time delay. In [11], Hannaford and Ryu proposed a passivity based model-insensitive approach that measures the total energy of the system and damps excess energy by injecting a variable damping, which was then extended in [30].

In this paper, the work in [25] is extended so that it is applicable for the control of both teleoperator and haptic systems. Two controllers are developed for nonlinear haptic and teleoperator systems that target coordination of the master and slave. The first controller is proven to yield a semi-global asymptotic result in the presence of parametric uncertainty in the master and slave dynamic models provided the user and environmental input forces are measurable; henceforth, referred to as the MIF, (measurable input force) controller. The second controller yields a global asymptotic result despite unmeasurable user and environmental input forces (UMIF) provided the dynamic models of the master and slave systems are known. This paper differs from [25], in that the transformation and target system development are both modified to allow the master system's impedance, felt by the user, to be adjusted so that it closely matches that of a desired target system operating in a remote environment. This work also provides the encoding of a velocity field assist mechanism to provide the user help in controlling the slave system in completing a predefined contour following task. To achieve these control objectives, a continuous nonlinear integral feedback controller/observer (see [28] and [36]) is exploited to compensate for the lack of master and slave dynamics information or user and environmental force measurements. For each controller, Lyapunov-based techniques are used to prove that the controller development implements a stable coordinated haptic/teleoperator system with the optional assist mechanism enabled. When this mechanism is disabled, the subsequent analysis proves the controller development implements a stable passively coordinated haptic/teleoperator system. The passivity objective is motivated to ensure the safety of the user and the environment when in contact with the haptic/teleoperator system. Simulation results are presented for proof of concept for both controllers.

2 System Model

The mathematical model for a $2n$-DOF nonlinear haptic/teleoperator system consisting of a revolute n-DOF master and a revolute n-DOF slave system are assumed to have the following forms

$$M_1(x_m)\ddot{x}_m + N_1(x_m, \dot{x}_m) = T_1 + F_H \quad (1)$$

$$M_2(x_s)\ddot{x}_s + N_2(x_s, \dot{x}_s) = T_2 + F_E. \quad (2)$$

In (1) and (2), $x_m(t)$, $\dot{x}_m(t)$, $\ddot{x}_m(t) \in \mathbb{R}^n$ denote the task-space position, velocity, and acceleration for the master system and $x_s(t)$, $\dot{x}_s(t)$, $\ddot{x}_s(t)$ denote the task-space position, velocity, and acceleration for the slave system, $M_1(x_m)$, $M_2(x_s) \in \mathbb{R}^{n\times n}$ represent the inertia effects, $N_1(x_m, \dot{x}_m)$, $N_2(x_s, \dot{x}_s) \in \mathbb{R}^n$ represent other dynamic effects, $T_1(t)$, $T_2(t) \in \mathbb{R}^n$ represent the control input vectors, $F_H(t) \in \mathbb{R}^n$ represents the user input force, and $F_E(t) \in \mathbb{R}^n$ represents the input force from the physical or virtual environment. End-effector positions $x_m(t)$ and $x_s(t)$ can be decomposed as follows

$$x_m \triangleq \begin{bmatrix} x_{mp}^T & x_{mr}^T \end{bmatrix}^T \qquad x_s \triangleq \begin{bmatrix} x_{sp}^T & x_{sr}^T \end{bmatrix}^T$$

where $x_{mp}(t), x_{sp}(t) \in \mathbb{R}^p$ represent position vectors and $x_{mr}(t), x_{sr}(t) \in \mathbb{R}^r$ represent orientation angle vectors, where the integers p and r satisfy $p + r = n$. The subsequent development utilizes the property that the master and slave inertia matrices are positive definite, symmetric and satisfies the following inequalities [23]

$$m_{1i}\|\xi\|^2 \le \xi^T M_i(\cdot)\xi \le m_{2i}\|\xi\|^2 \quad (3)$$

$\forall \xi \in \mathbb{R}^n$ and $i = 1, 2$ where $m_{1i}, m_{2i} \in \mathbb{R}$ are positive constants, and $\|\cdot\|$ denotes the Euclidean norm. To achieve the control objectives, the subsequent development is derived based on the assumption that $x_m(t)$, $x_s(t)$, $\dot{x}_m(t)$, $\dot{x}_s(t)$ are measurable, and $M_i(\cdot)$, $N_i(\cdot)$ are second order differentiable for $i = 1, 2$.

Assumption 1 The user input force and the environmental force along with their first and second time derivatives, $F_H(t)$, $\dot{F}_H(t)$, $\ddot{F}_H(t)$, $F_E(t)$, $\dot{F}_E(t)$, and $\ddot{F}_E(t)$ are bounded (see [15] and [17] for the precedence of this type of assumption).

3 MIF Control Development

For the MIF controller development, the following analysis will prove a semi-global asymptotic result despite para-

metric uncertainty in the master and slave system dynamic models provided the user and the physical or virtual environmental input forces are measurable. It should be noted that for many types of virtual slave systems, the dynamic model of the virtual slave is known *a priori*; however; unstructured uncertainties in the dynamic model are common for teleoperator slave systems.

3.1 Control Objective and Model Transformation

A control objective for haptic and teleoperator systems is to ensure the coordination between the master and the slave systems and to meet the tracking objective in the following sense

$$x_s(t) \rightarrow x_m(t) \text{ as } t \rightarrow \infty \tag{4}$$

$$x_m(t) \rightarrow \xi_d(t) \text{ as } t \rightarrow \infty \tag{5}$$

where $\xi_d(t) \in \mathbb{R}^n$ is a subsequently designed desired trajectory. Another sub-control objective is to guarantee that the closed-loop system remains passive with respect to the user and the physical/virtual environmental power in the following sense [15]

$$\int_{t_0}^{t} \left(\dot{x}_m^T(\tau) F_H(\tau) + \dot{x}_s^T(\tau) F_E(\tau) \right) d\tau \geq -c_1^2 \tag{6}$$

where $c_1 \in \mathbb{R}$ is a bounding constant. The passivity objective is motivated to ensure the safety of the user and the physical environment [15]. The final objective is that all signals are required to remain bounded within the closed-loop system. It should be noted that, the passivity objective is not met when the subsequently presented user assist mechanism is enabled.

To facilitate the subsequent development, an invertible transformation is defined that encodes the control objectives as follows

$$x \triangleq S \begin{bmatrix} x_m^T & x_s^T \end{bmatrix}^T \tag{7}$$

where $x(t) \in \mathbb{R}^{2n}$ and $S \in \mathbb{R}^{2n \times 2n}$ is defined as follows

$$S \triangleq \begin{bmatrix} I_n & 0_{nxn} \\ I_n & -I_n \end{bmatrix} \tag{8}$$

where $I_n \in \mathbb{R}^{n \times n}$ denotes the identity matrix, $0_{nxn} \in \mathbb{R}^{n \times n}$ denotes a matrix of zeros, and it is noted that $S^{-1} = S$. After utilizing the transformation defined in (7), the dynamic models of the haptic/teleoperator systems given in (1) and (2) can be combined as follows

$$\bar{M}\ddot{x} + \bar{N} = \bar{T} + \bar{F} \tag{9}$$

where $\bar{N}(x, \dot{x})$, $\bar{T}(t)$, $\bar{F}(t) \in \mathbb{R}^{2n}$ and $\bar{M}(x) \in \mathbb{R}^{2n \times 2n}$ are defined as follows

$$\bar{M} \triangleq S^{-T} \begin{bmatrix} M_1 & 0_{nxn} \\ 0_{nxn} & M_2 \end{bmatrix} S^{-1} \tag{10}$$

$$\bar{N} \triangleq S^{-T} \begin{bmatrix} N_1^T & N_2^T \end{bmatrix}^T \tag{11}$$

$$\bar{T} \triangleq S^{-T} \begin{bmatrix} T_1^T & T_2^T \end{bmatrix}^T \tag{12}$$

$$\bar{F} \triangleq S^{-T} \begin{bmatrix} F_H^T & F_E^T \end{bmatrix}^T. \tag{13}$$

The subsequent development utilizes the property that $\bar{M}(x)$ is positive definite, symmetric and satisfies the following inequalities [23]

$$\bar{m}_1 \|\xi\|^2 \leq \xi^T \bar{M}(x) \xi \leq \bar{m}_2 \|\xi\|^2 \tag{14}$$

$\forall \xi \in \mathbb{R}^{2n}$ where $\bar{m}_1$, $\bar{m}_2 \in \mathbb{R}$ are positive constants. By utilizing the assumption that $M_i(\cdot)$, $N_i(\cdot)$ are second order differentiable for $i = 1, 2$, it is clear that $\bar{M}(\cdot)$ and $\bar{N}(\cdot)$ are also second order differentiable.

To facilitate the development of the error system, the filtered tracking error signal, denoted by $r(t) \in \mathbb{R}^{2n}$, is defined as follows

$$r \triangleq \dot{e}_2 + \alpha_1 e_2 \tag{15}$$

where $e_2(t) \in \mathbb{R}^{2n}$ is defined as follows

$$e_2 \triangleq \dot{e}_1 + \alpha_2 e_1 \tag{16}$$

where α_1, $\alpha_2 \in \mathbb{R}$ are positive control gains, and $e_1(t) \in \mathbb{R}^{2n}$ is defined as follows

$$e_1 \triangleq x_d - x. \tag{17}$$

The error signal $e_1(t)$ can be decomposed as follows

$$e_1 \triangleq \begin{bmatrix} e_{11}^T & e_{12}^T \end{bmatrix}^T \tag{18}$$

where $e_{11}(t) \in \mathbb{R}^n$ represents the master system tracking error, and $e_{12}(t) \in \mathbb{R}^n$ represents the coordination error. In (17), $x_d(t) \in \mathbb{R}^{2n}$ is defined as follows

$$x_d \triangleq \begin{bmatrix} \xi_d^T & 0_n^T \end{bmatrix}^T \tag{19}$$

where $0_n \in \mathbb{R}^n$ denotes a vector of zeros. Based on the definition of $x(t)$ in (7) and $e_1(t)$ in (17), it is clear that if $\|e_1(t)\| \rightarrow 0$ then $x_s(t) \rightarrow x_m(t)$ and $x_m(t) \rightarrow \xi_d(t)$.

The desired trajectory $\xi_d(t)$ introduced in (5) is generated by the following second-order coupled dynamic target system

$$\dot{\xi}_d = \gamma \begin{bmatrix} \varphi^T(\xi_p) & 0_r^T \end{bmatrix}^T + \eta_d \tag{20}$$

$$M_T \dot{\eta}_d + B_T \eta_d + K_T \lambda_d = F \tag{21}$$

where $\eta_d(t) \in \mathbb{R}^n$ is an auxiliary filter signal, M_T, B_T, $K_T \in \mathbb{R}^{n \times n}$ are constant positive definite, diagonal matrices, $\varphi(\cdot) \in \mathbb{R}^p$ is a velocity field function [24] that encodes the user assist mechanism, $0_r \in \mathbb{R}^r$ denotes a vector of zeros, γ is a constant gain that is either 0 or 1. It should be noted that, when $\gamma = 0$, the user assist mechanism is disabled, and when $\gamma = 1$, then the user assist mechanism is enabled. In (21), $F(t) \in \mathbb{R}^n$ is defined as follows

$$F \triangleq F_H + F_E. \tag{22}$$

Also, in (21) the term $\lambda_d(t) \in \mathbb{R}^n$ is defined as follows

$$\lambda_d \triangleq \xi_d - \gamma \begin{bmatrix} \int_{t_0}^{t} \varphi^T(\xi_p(\tau)) d\tau & 0_r^T \end{bmatrix}^T \tag{23}$$

where $\xi_d(t)$ is generated by the differential equation of (20), and can be decomposed as follows

$$\xi_d \triangleq \begin{bmatrix} \xi_p^T & \xi_r^T \end{bmatrix}^T \tag{24}$$

where $\xi_p(t) \in \mathbb{R}^p$ represents a position vector, and $\xi_r(t) \in \mathbb{R}^r$ represents an orientation angle vector.

Remark 1 *Velocity fields have been utilized in previous control literature, see [2] and [24] for their definition and application. The velocity field function in (20) is integrated to assist the user in executing a remote task (i.e., tracking a circular contour). It is assumed that the velocity field function is designed such that $\varphi(\cdot)$, $\dot{\varphi}(\cdot)$, $\ddot{\varphi}(\cdot)$ and $\dddot{\varphi}(\cdot)$ are bounded provided that their arguments are bounded.*

Remark 2 *The velocity field function $\varphi(\cdot)$ is assumed to be designed such that, from (20), if $\eta_d(t) \in \mathcal{L}_\infty$ then $\xi_d(t)$, $\dot{\xi}_d(t) \in \mathcal{L}_\infty$. Based on this assumption and the analysis in Appendix A, it is easy to show that all signals in dynamic target system given in (20) and (21) are bounded, and that the higher order derivatives are also bounded.*

Remark 3 *It should be noted that, when the user assist mechanism is disabled, (i.e., $\gamma = 0$) the target system defined by (20) and (21), becomes a standard impedance model as follows*

$$M_T\ddot{\xi}_d + B_T\dot{\xi}_d + K_T\xi_d = F. \tag{25}$$

3.2 Closed-Loop Error System

Based on the assumption that the user forces $F_H(t)$, and the physical/virtual environmental forces $F_E(t)$, are measurable, the control input $\bar{T}(t)$ of (9) is designed as follows

$$\bar{T} \triangleq \bar{u} - \bar{F} \tag{26}$$

where $\bar{u}(t) \in \mathbb{R}^{2n}$ is a subsequently designed auxiliary control input. Substituting (26) into (9) results in the following simplified dynamic system

$$\bar{M}\ddot{x} + \bar{N} = \bar{u}. \tag{27}$$

After taking the time derivative of (15) and premultiplying by $\bar{M}(x)$, the following expression can be derived

$$\bar{M}\dot{r} = \bar{M}\,\dddot{x}_d + \dot{\bar{M}}\ddot{x} + \dot{\bar{N}} - \dot{\bar{u}} + \alpha_2\bar{M}\ddot{e}_1 + \alpha_1\bar{M}\dot{e}_2 \tag{28}$$

where (16), (17), and the time derivative of (27) were utilized. To facilitate the subsequent analysis, the expression in (28) can be arranged as follows

$$\bar{M}\dot{r} = \tilde{N} + N_d - e_2 - \dot{\bar{u}} - \frac{1}{2}\dot{\bar{M}}\,r \tag{29}$$

where $\tilde{N}(x, \dot{x}, \ddot{x}, t) \in \mathbb{R}^{2n}$ is defined as follows

$$\tilde{N} \triangleq N - N_d \tag{30}$$

where $N(x, \dot{x}, \ddot{x}, t) \in \mathbb{R}^{2n}$ is defined as follows

$$\begin{aligned} N \triangleq\ & \bar{M}\,\dddot{x}_d + \dot{\bar{M}}\,\ddot{x} + \alpha_2\bar{M}\ddot{e}_1 \\ & + \alpha_1\bar{M}\dot{e}_2 + e_2 + \dot{\tilde{N}} + \frac{1}{2}\dot{\bar{M}}\,r \end{aligned} \tag{31}$$

and $N_d(t) \in \mathbb{R}^{2n}$ is defined as follows

$$\begin{aligned} N_d &\triangleq N|_{x=x_d,\ \dot{x}=\dot{x}_d,\ \ddot{x}=\ddot{x}_d} \\ &= \bar{M}(x_d)\,\dddot{x}_d + \dot{\bar{M}}(x_d, \dot{x}_d)\,\ddot{x}_d + \dot{\tilde{N}}(x_d, \dot{x}_d, \ddot{x}_d). \end{aligned} \tag{32}$$

Remark 4 *After utilizing (19), (32) and the fact that we show in Appendix A, then $\|N_d(t)\|$ and $\left\|\dot{N}_d(t)\right\|$ can be upper bounded as follows*

$$\|N_d(t)\| \le \varsigma_1 \qquad \left\|\dot{N}_d(t)\right\| \le \varsigma_2 \tag{33}$$

where ς_1, $\varsigma_2 \in \mathbb{R}$ are known positive constants.

To achieve the stated control objectives, the auxiliary control input $\bar{u}(t)$ introduced in (26) is designed as follows

$$\begin{aligned} \bar{u} \triangleq\ & (k_s + 1)\left[e_2(t) - e_2(t_0) + \alpha_1\int_{t_0}^{t} e_2(\tau)\,d\tau\right] \\ & + (\beta_1 + \beta_2)\int_{t_0}^{t} sgn(e_2(\tau))\,d\tau \end{aligned} \tag{34}$$

where k_s, β_1, $\beta_2 \in \mathbb{R}$ are positive control gains, and $sgn(\cdot)$ denotes the vector signum function. The term $e_2(t_0)$ in (34) is used to ensure that $\bar{u}(t_0) = 0_{2n}$ where $0_{2n} \in \mathbb{R}^{2n}$ denotes a vector of zeros. The time derivative of (34) is obtained as follows

$$\dot{\bar{u}} = (k_s + 1)\,r + (\beta_1 + \beta_2)\,sgn(e_2) \tag{35}$$

where (15) was utilized. Substituting (35) into (29) results in the following closed-loop error system

$$\begin{aligned} \bar{M}\dot{r} =\ & -(k_s + 1)\,r - (\beta_1 + \beta_2)\,sgn(e_2) \\ & + \tilde{N} + N_d - e_2 - \frac{1}{2}\dot{\bar{M}}\,r. \end{aligned} \tag{36}$$

3.3 Stability Analysis

Theorem 1 *The controller given in (26) and (34) guarantees that all the system signals are bounded under the closed-loop operation and that coordination between the master and the slave systems, and the tracking objective are met in the sense that*

$$x_s(t) \rightarrow x_m(t) \ \text{ as } t \to \infty \tag{37}$$

$$x_m(t) \rightarrow \xi_d(t) \ \text{ as } t \to \infty \tag{38}$$

provided the control gain β_1 introduced in (34) is selected to satisfy the following sufficient condition

$$\beta_1 > \varsigma_1 + \frac{1}{\alpha_1}\varsigma_2 \tag{39}$$

where ς_1 and ς_2 were introduced in (33), the control gains α_1 and α_2 are selected greater than 2, and k_s is selected sufficiently large relative to the system's initial conditions.

Proof. See Appendix B.

Theorem 2 *The controller given in (26) and (34) guarantees the closed-loop system is passive with respect to the user and the physical/virtual environmental power when the user assist mechanism is disabled (i.e., $\gamma = 0$).*

Proof. See Appendix C.

4 UMIF Control Development

For the UMIF controller development, the following analysis will prove a global asymptotic result despite unmeasurable user and environmental input forces provided the dynamic models of the master and slave systems are known. Assumption 1 is also utilized for the subsequent development. It should be noted that, for many types of virtual slave systems, the virtual environmental forces are measurable; however, the user input force may not be measurable.

4.1 Control Objective and Model Transformation

A control objective for haptic and teleoperator systems is to guarantee coordination between the master and the slave systems and to meet the tracking objective in the following sense

$$x_s(t) \rightarrow x_m(t) \text{ as } t \rightarrow \infty \tag{40}$$

$$x_m(t) \rightarrow \xi_1(t) \text{ as } t \rightarrow \infty \tag{41}$$

where $\xi_1(t) \in \mathbb{R}^n$ is a subsequently designed desired trajectory. Another sub-control objective is to guarantee that the system remains passive with respect to the user and the environmental power as in (6). It should be noted that the passivity objective is not met when the user assist mechanism is enabled. The final objective is that all signals are required to remain bounded within the closed-loop system.

To facilitate the subsequent development, an invertible transformation is defined that encodes the control objectives as follows

$$x \triangleq S \begin{bmatrix} x_m \\ x_s \end{bmatrix} + \begin{bmatrix} 0_n \\ \xi_2 \end{bmatrix} \tag{42}$$

where $x(t) \in \mathbb{R}^{2n}$ and $\xi_2(t) \in \mathbb{R}^n$ is a subsequently defined desired trajectory, and $S \in \mathbb{R}^{2n \times 2n}$ was defined in (8). After utilizing the transformation defined in (42), the dynamic models of the haptic/teleoperator system given in (1) and (2) can be combined as follows

$$\bar{M}\ddot{x} - \bar{M} \begin{bmatrix} 0_n \\ \ddot{\xi}_2 \end{bmatrix} + \bar{N} = \bar{T} + \bar{F} \tag{43}$$

where $\bar{M}(x)$, $\bar{N}(x, \dot{x})$, $\bar{T}(t)$, and $\bar{F}(t)$ were defined in (10)-(13).

The filtered tracking error signal denoted by $r(t) \in \mathbb{R}^{2n}$ is defined as follows

$$r \triangleq \dot{e}_2 + e_2 \tag{44}$$

where $e_2(t) \in \mathbb{R}^{2n}$ is defined as follows

$$e_2 \triangleq \bar{M}(\dot{e}_1 + \alpha e_1) \tag{45}$$

where $\alpha \in \mathbb{R}$ is a positive control gain, and $e_1(t) \in \mathbb{R}^{2n}$ is defined as follows

$$e_1 \triangleq \xi_d - x \tag{46}$$

where $\xi_d(t)$ is a subsequently defined desired trajectory. The error signal $e_1(t)$ can be decomposed as follows

$$e_1 \triangleq \begin{bmatrix} e_{11}^T & e_{12}^T \end{bmatrix}^T \tag{47}$$

where $e_{11}(t) \in \mathbb{R}^n$ represents the master system tracking error, and $e_{12}(t) \in \mathbb{R}^n$ represents the coordination error.

To compensate for the unmeasurable user and physical/virtual environmental forces, a nonlinear force observer is designed subsequently. This nonlinear observer is utilized in driving the target system, thus requiring a $2n$-dimensional system. As a result of this fact, the desired trajectory, defined as $\xi_d(t) \in \mathbb{R}^{2n}$, is generated by the following second order coupled dynamic target system[1]

$$\dot{\xi}_d = \gamma \begin{bmatrix} \varphi^T(\xi_{1p}) & 0_s^T \end{bmatrix}^T + \eta_d \tag{48}$$

$$M_T \dot{\eta}_d + B_T \eta_d + K_T \lambda_d = \left(\bar{M} M_T^{-1}\right)^{-1} \hat{F} \tag{49}$$

where $\eta_d(t) \in \mathbb{R}^{2n}$ is an auxiliary filter signal, $\bar{M}(x)$ was defined in (10), M_T, B_T and $K_T \in \mathbb{R}^{2n \times 2n}$ represent constant, positive definite, diagonal matrices, $\hat{F}(t) \in \mathbb{R}^{2n}$ is a subsequently designed nonlinear observer, $\varphi(\cdot) \in \mathbb{R}^p$ was introduced in Section 3.1, $0_s \in \mathbb{R}^s$ denotes a vector of zeros where $s + p = 2n$, and γ is a constant gain that is either 0 or 1. It should be noted that, when $\gamma = 0$, the user assist mechanism is disabled, and when $\gamma = 1$, then the user assist mechanism is enabled. In (49), the term $\lambda_d(t) \in \mathbb{R}^{2n}$ is defined as follows

$$\lambda_d \triangleq \xi_d - \gamma \begin{bmatrix} \int_{t_0}^{t} \varphi^T(\xi_{1p}(\tau))\, d\tau & 0_s^T \end{bmatrix}^T \tag{50}$$

[1] For the existence of $\left(\bar{M} M_T^{-1}\right)^{-1}$ see Appendix G.

where $\xi_d(t) \triangleq \left[\begin{array}{cc} \xi_1^T & \xi_2^T \end{array}\right]^T$ is generated by the differential equation given in (48) where $\xi_1(t), \xi_2(t) \in \mathbb{R}^n$. The desired trajectory for the master system denoted by $\xi_1(t)$, can be decomposed as follows

$$\xi_1 \triangleq \left[\begin{array}{cc} \xi_{1p}^T & \xi_{1r}^T \end{array}\right]^T \tag{51}$$

where $\xi_{1p}(t) \in \mathbb{R}^p$ represents a position vector, and $\xi_{1r}(t) \in \mathbb{R}^r$ represents an orientation angle vector.

Remark 5 *The velocity field function $\varphi(\cdot)$ is assumed to be designed such that, from (48), if $\eta_d(t) \in \mathcal{L}_\infty$ then $\xi_d(t)$, $\dot{\xi}_d(t) \in \mathcal{L}_\infty$. Subsequent analysis will prove that $\hat{F}(t) \in \mathcal{L}_\infty$. After utilizing these facts along with (14), the analysis in Appendix F proves that all signals in the dynamic target system given in (48) and (49) are bounded.*

Remark 6 *Although the desired trajectory dynamics defined in (48) and (49) generated a $2n$-dimensional signal, it should be noted that the master system tracks an n-dimensional signal, denoted as $\xi_1(t)$. The use of a $2n$-dimensional desired trajectory generator is a consequence of the fact that both the user input force and the physical/virtual environmental force are unmeasurable, and hence, a $2n$-dimensional nonlinear force observer must be utilized to drive the target system as defined in (49). From the definition of the transformation and the error signal $e_1(t)$ (see (42) and (46)), it is clear that additional set of desired trajectory dynamics, denoted by $\xi_2(t)$, are eliminated in the error system development.*

Remark 7 *It should be noted that, when the user assist mechanism is disabled (i.e., $\gamma = 0$), then the target system defined by (48) and (49), becomes an impedance model described as follows*

$$M_T\ddot{\xi}_d + B_T\dot{\xi}_d + K_T\xi_d = \left(\bar{M}M_T^{-1}\right)^{-1}\hat{F}. \tag{52}$$

4.2 Closed-Loop Error System

To develop the closed-loop error system for $r(t)$, error system dynamics for $e_1(t)$ and $e_2(t)$ are derived first. After taking the second time derivative of (46) and premultiplying by $\bar{M}(x)$, the following expression can be derived

$$\begin{aligned} \bar{M}\ddot{e}_1 &= \hat{F} - \left(\bar{M}M_T^{-1}\right)(B_T\eta_d + K_T\lambda_d) \\ &\quad -\bar{M}\left[\begin{array}{c} 0_n \\ \ddot{\xi}_2 \end{array}\right] + \bar{N} - \bar{T} - \bar{F} \\ &\quad +\gamma\bar{M}\frac{d}{dt}\left(\left[\begin{array}{cc} \varphi^T(\xi_{1p}) & 0_s^T \end{array}\right]^T\right) \end{aligned} \tag{53}$$

where (43), (48) and (49) were utilized. Based on the assumption of exact model knowledge, the control input $\bar{T}(t)$ is designed as follows

$$\begin{aligned} \bar{T} &\triangleq \bar{T}_1 - \left(\bar{M}M_T^{-1}\right)(B_T\eta_d + K_T\lambda_d) - \bar{M}\left[\begin{array}{c} 0_n \\ \ddot{\xi}_2 \end{array}\right] \\ &\quad +\bar{N} + \gamma\bar{M}\frac{d}{dt}\left(\left[\begin{array}{cc} \varphi^T(\xi_{1p}) & 0_s^T \end{array}\right]^T\right) \end{aligned} \tag{54}$$

where $\bar{T}_1(t) \in \mathbb{R}^{2n}$ is a subsequently designed auxiliary control input. Substituting (54) into (53) results in the following simplified expression

$$\bar{M}\ddot{e}_1 = \hat{F} - \bar{F} - \bar{T}_1. \tag{55}$$

The time derivative of $e_2(t)$ in (45) can be obtained as follows

$$\dot{e}_2 = \dot{\bar{M}}\,\dot{e}_1 + \alpha\,\dot{\bar{M}}\,e_1 + \alpha\bar{M}\dot{e}_1 + \dot{\hat{F}} - \dot{\bar{F}} - \dot{\bar{T}}_1 \tag{56}$$

where (55) was utilized. Based on (56), the auxiliary control input $\bar{T}_1(t)$ is designed as follows

$$\bar{T}_1 \triangleq \dot{\bar{M}}\,\dot{e}_1 + \alpha\,\dot{\bar{M}}\,e_1 + \alpha\bar{M}\dot{e}_1. \tag{57}$$

After substituting (57) into (56), the following simplified expression is obtained

$$\dot{e}_2 = \dot{\hat{F}} - \dot{\bar{F}}. \tag{58}$$

Taking the time derivative of (58) results in the following expression

$$\ddot{e}_2 = \ddot{\hat{F}} - \ddot{\bar{F}}\,. \tag{59}$$

The error system dynamics for $r(t)$ can be derived by taking the time derivative of (44)

$$\dot{r} = r - e_2 + \dot{\hat{F}} - \dot{\bar{F}} \tag{60}$$

where (44) and (59) were both utilized. To achieve the stated control objectives, the proportional-integral like nonlinear observer $\hat{F}(t)$ introduced in (49) is designed as follows

$$\begin{aligned} \hat{F} &\triangleq -(k_s+1)\left[e_2(t) - e_2(t_0) + \int_{t_0}^{t} e_2(\tau)\,d\tau\right] \\ &\quad -(\beta_1+\beta_2)\int_{t_0}^{t} sgn(e_2(\tau))\,d\tau \end{aligned} \tag{61}$$

where k_s, β_1, and $\beta_2 \in \mathbb{R}$ are positive control gains. The term $e_2(t_0)$ is used to ensure that $\hat{F}(t_0) = 0_{2n}$. The time derivative of (61) is obtained as follows

$$\dot{\hat{F}} = -(k_s+1)\,r - (\beta_1+\beta_2)\,sgn(e_2) \tag{62}$$

where (44) was utilized. Substituting (62) into (60) results in the following closed-loop error system

$$\dot{r} = -e_2 - \dot{\bar{F}} - k_s r - (\beta_1+\beta_2)\,sgn(e_2)\,. \tag{63}$$

Remark 8 *After utilizing (13) and Assumption 1, then $\left\|\dot{\bar{F}}(t)\right\|$ and $\left\|\ddot{\bar{F}}(t)\right\|$ can be upper bounded as follows*

$$\left\|\dot{\bar{F}}(t)\right\| \le \varsigma_3 \qquad \left\|\ddot{\bar{F}}(t)\right\| \le \varsigma_4 \tag{64}$$

where ς_3, $\varsigma_4 \in \mathbb{R}$ denote positive bounding constants.

4.3 Stability Analysis

Theorem 3 *The controller given in (54) and (57) guarantees that all signals are bounded under closed-loop operation and that coordination between the master and the slave systems, and the tracking objective are met in the sense that*

$$x_s(t) \rightarrow x_m(t) \ \ as\ t \rightarrow \infty \tag{65}$$

$$x_m(t) \rightarrow \xi_1(t) \ \ as\ t \rightarrow \infty \tag{66}$$

provided the control gain β_1, introduced in (61) is selected to satisfy the sufficient condition

$$\beta_1 > \varsigma_3 + \varsigma_4, \tag{67}$$

where ς_3 and ς_4 were introduced in (64).

Proof. See Appendix D.

Theorem 4 *The controller given in (54) and (57) guarantees that the haptic/teleoperator system is passive with respect to the user and the physical/virtual environmental power when the user assist mechanism is disabled (i.e., $\gamma = 0$).*

Proof. See Appendix E.

5 Conclusions

Two controllers were developed for nonlinear haptic and teleoperator systems that target coordination of the master and slave. The first controller was proven to yield a semi-global asymptotic result in the presence of parametric uncertainty in the master and slave dynamic models provided the user and environmental input forces are measurable. The second controller was proven to yield a global asymptotic result despite unmeasurable user and environmental input forces provided the dynamic models of the master and slave are known. A transformation along with an adjustable target system were utilized that allows the master system's impedance to be adjusted so that matches a desired target system operating in a remote physical/virtual environment. This work also presented an optional strategy to encode a velocity field assist mechanism that provides the user of the system help in controlling the slave system in completing a pre-defined contour following task. For each controller, Lyapunov-based techniques were used to prove the control development implements a stable coordinated teleoperator/haptic system with a user assist mechanism. When the optional velocity field assist mechanism is disabled, the analysis proved the control development implements a stable passively coordinated teleoperator/haptic system. Simulation results demonstrated proof of concept for both controllers (see appendices I and J).

References

[1] R. J. Anderson and M. W. Spong, "Bilateral Control of Teleoperators with Time Delay," IEEE Trans. on Automatic Control, Vol. 34, No. 5, pp. 494-501 (1989).

[2] I. Cervantes, R. Kelly, J. Alvarez-Ramirez, and J. Moreno, "A Robust Velocity Field Control," IEEE Trans. on Control System Technology, Vol. 10, No. 6, pp. 888-894, (2002).

[3] N. Chopra, M. W. Spong, S. Hirche, and M. Buss, "Bilateral Teleoperation over the Internet: the Time Varying Delay Problem," Proc. IEEE American Control Conference, June 4-6, Denver, CO, 2003, pp. 155-160.

[4] N. Chopra, M. W. Spong, R. Ortega, and N. E. Barabanov, "On Position Tracking in Bilateral Teleoperation," Proc. IEEE American Control Conference, June 30-July 2, Boston, MA, 2004, pp. 5244-5249.

[5] N. Chopra, M. W. Spong, and R. Lozano, "Adaptive Coordination Control of Bilateral Teleoperators with Time Delay," Proc. of IEEE Conference on Decision and Control, December 14-17, Nassau, Bahamas, 2004, pp. 4540-4547.

[6] J. E. Colgate, "Robust Impedance Shaping Telemanipulation," IEEE Trans. on Robotics and Automation, Vol. 9, No. 4, pp. 374-384 (1993).

[7] M. Corless and G. Leitmann, "Continuous State Feedback Guaranteeing Uniform Ultimate Boundedness for Uncertain Dynamic Systems," IEEE Trans. on Automatic Control, Vol. 26, No. 5, pp. 1139-1144 (1981).

[8] E. L. Faulring, K. M. Lynch, J. E. Colgate and M. A. Peshkin, "Haptic Interaction With Constrained Dynamic Systems," Proc. IEEE Int. Conf. on Robotics and Automation, April 18-22, Barcelona, Spain, 2005, pp. 2458-2464.

[9] K. B. Fite, L. Shao, and M. Goldfarb, "Loop shaping for transparency and stability robustness in bilateral telemanipulation," IEEE Trans. on Robotics and Automation, Vol. 20, No. 3, pp. 620-624 (2004).

[10] B. Hannaford, "A Design Framework for Teleoperators with Kinesthetic Feedback," IEEE Trans. on Robotics and Automation, Vol. 5, No. 4, pp. 426-434 (1989).

[11] B. Hannaford and J. -H. Ryu, "Time domain passivity control of haptic interfaces," IEEE Trans. on Robotics and Automation, Vol. 18, No. 1, pp. 1-10 (2002).

[12] K. Hashtrudi-Zaad and S. E. Salcudean, "Adaptive transparent impedance reflecting teleoperation," Proc. IEEE Int. Conf. on Robotics and Automation, April 22-28, Minneapolis, MN, 1996, pp. 1369-1374.

[13] H. Khalil, Nonlinear Systems, Third Edition, Upper Saddle River, NJ: Prentice-Hall, Inc., 2002.

[14] D. A. Lawrence, "Stability and Transparency in Bilateral Teleoperation," IEEE Trans. on Robotics and Automation, Vol. 9, No. 5, pp. 624-637 (1993).

[15] D. Lee and P. Y. Li, "Passive Coordination Control of Nonlinear Bilateral Teleoperated Manipulators," Proc. IEEE Int. Conf. Robotics and Automation, May 11-15, Washington, DC, 2002, pp. 3278-3283.

[16] D. Lee and P. Y. Li, "Passive tool dynamics rendering for nonlinear bilateral teleoperated manipulators," Proc. IEEE Int. Conf. Robotics and Automation, May 11-15, Washington, DC, 2002, pp. 3284-3289.

[17] D. Lee and P. Y. Li, "Passive Bilateral Feedforward Control of Linear Dynamically Similar Teleoperated Manipulators," IEEE Trans. on Robotics and Automation, Vol. 19, No. 3, pp. 443-456 (2003).

[18] D. Lee and P. Y. Li, "Toward robust passivity: a passive control implementation structure for mechanical teleoperators," Proc. IEEE VR Symposium on Haptic Interfaces for Virtual Environment and Teleoperator Systems, March 22-23, Los Angeles, CA, 2003, pp. 132-139.

[19] D. Lee and P. Y. Li, "Passive bilateral control and tool dynamics rendering for nonlinear mechanical teleoperators," IEEE Trans. on Robotics, Vol. 21, No. 5, pp. 936-951 (2005).

[20] D. Lee and M. W. Spong, "Bilateral Teleoperation of Multiple Cooperative Robots over Delayed Communication Networks: Theory," Proc. of IEEE Int. Conf. Robotics and Automation, April 18-22, Barcelona, Spain, 2005, pp. 360-365.

[21] D. Lee, O. Martinez-Palafox, and M. W. Spong, "Bilateral Teleoperation of Multiple Cooperative Robots over Delayed Communication Networks: Application," Proc. of IEEE Int. Conf. Robotics and Automation, April 18-22, Barcelona, Spain, 2005, pp. 366-371.

[22] H. -K. Lee and M. J. Chung, "Adaptive controller of a master-slave system for transparent teleoperation," Journal of Robotic Systems, Vol. 15, No. 8, pp. 465-475 (1998).

[23] F. L. Lewis, D. M. Dawson, and C. T. Abdallah, Robot Manipulator Control: Theory and Practice, New York, NY: Marcel Dekker, Inc., 2004.

[24] P. Li and R. Horowitz, Passive Velocity Field Control of Mechanical Manipulators, IEEE Trans. on Robotics and Automation, Vol. 15, No. 4, pp. 751-763, (1999).

[25] M. McIntyre, W. Dixon, D. Dawson, and E. Tatlicioglu, "Passive Coordination of Nonlinear Bilateral Teleoperated Manipulators," Robotica, accepted, to appear, 2006.

[26] G. Niemeyer, and J. -J. E. Slotine, "Stable Adaptive Teleoperation," IEEE Journal of Oceanic Engineering, Vol. 16, No. 1, pp. 152-162 (1991).

[27] G. Niemeyer, and J. -J. E. Slotine, "Designing Force Reflecting Teleoperators with Large Time Delays to Appear as Virtual Tools," Proc. IEEE Int. Conf. Robotics and Automation, April 20-25, Albuquerque, NM, 1997, pp. 2212-2218.

[28] Z. Qu and J. -X. Xu, "Model-Based Learning Controls and Their Comparisons Using Lyapunov Direct Method," Asian Journal of Control, Vol. 4, No. 1, pp. 99-110 (2002).

[29] J. -H. Ryu and D. -S. Kwon, "A Novel Adaptive Bilateral Control Scheme Using Similar Closed-loop Dynamic Characteristics of Master/Slave Manipulators," Journal of Robotic Systems, Vol. 18, No. 9, pp. 533-543, (2001).

[30] J. -H. Ryu, C. Preusche, B. Hannaford, and G. Hirzinger, "Time domain passivity control with reference energy following," IEEE Trans. on Control Systems Technology, Vol. 13, No. 5, pp. 737-742 (2005).

[31] S. E. Salcudean, M. Zhu, W. -H. Zhu, and K. Hashtrudi-Zaad, "Transparent Bilateral Teleoperation Under Position and Rate Control," Int. Journal of Robotics Research, Vol. 19, No. 12, pp. 1185-1202 (2000).

[32] T. B. Sheridan, Telerobotics, Automation, and Human Supervisory Control, Cambridge, MA: MIT Press, 1992.

[33] M. Shi, G. Tao, H. Liu, and J. Hunter Downs, "Adaptive control of teleoperation systems," Proc. of IEEE Int. Conf. Decision and Control, December 7-10, Phoenix, AZ, 1999, pp. 791-796.

[34] M. W. Spong, and M. Vidyasagar, Robot Dynamics and Control, New York, NY: John Wiley & Sons, Inc., 1989.

[35] R. Q. Van der Linde, P. Lammertse, E. Frederiksen, B. Ruiter, "The HapticMaster, a new high-performance haptic interface," Proc. EuroHaptics, Edinburgh, U.K., 2002.

[36] B. Xian, M. S. de Queiroz, and D. M. Dawson, "A Continuous Control Mechanism for Uncertain Nonlinear Systems," Optimal Control, Stabilization, and Nonsmooth Analysis, Lecture Notes in Control and Information Sciences, Heidelberg, Germany: Springer-Verlag, pp. 251-262, 2004.

[37] Y. Yokokohji and T. Yoshikawa, "Bilateral Control of Master-Slave Manipulators for Ideal Kinesthetic Coupling-Formulation and Experiment," IEEE Trans. on Robotics and Automation, Vol. 10, No. 5, pp. 605-620 (1994).

[38] W. -H. Zhu and S. E. Salcudean, "Stability Guaranteed Teleoperation: An Adaptive Motion/Force Control Approach," IEEE Trans. on Automatic Control, Vol. 45, No. 11, pp. 1951-1969 (2000).

Appendices

A MIF Desired Trajectory Stability Analysis

To prove that $\xi_d(t)$, $\lambda_d(t)$, $\eta_d(t)$, $\dot{\eta}_d(t) \in \mathcal{L}_\infty$, let $V(t) \in \mathbb{R}$ denote the following function

$$V \triangleq V_1 + V_2 \tag{68}$$

where $V_1(t) \in \mathbb{R}$ denotes the following non-negative function

$$V_1 \triangleq \frac{1}{2}\eta_d^T M_T \eta_d + \frac{1}{2}\lambda_d^T K_T \lambda_d \tag{69}$$

where $\lambda_d(t)$, $\eta_d(t)$, M_T and K_T were introduced in (21). The expression given in (69) can be lower bounded by the auxiliary function, $V_2(\bar{x}) \in \mathbb{R}$, which is defined as follows

$$V_2 \triangleq 2\varepsilon \eta_d^T M_T \lambda_d \leq V_1 \tag{70}$$

where $\bar{x}(t) \in \mathbb{R}^{2n}$ is defined as follows

$$\bar{x} \triangleq \begin{bmatrix} \lambda_d^T & \eta_d^T \end{bmatrix}^T \tag{71}$$

and $\varepsilon \in \mathbb{R}$ is a positive bounding constant selected according to the following inequality

$$\varepsilon < \frac{\min\{\lambda_{\min}\{M_T\}, \lambda_{\min}\{K_T\}\}}{4\lambda_{\max}\{M_T\}} \tag{72}$$

where $\lambda_{\min}\{\cdot\}$ and $\lambda_{\max}\{\cdot\}$ denote the minimum and maximum eigenvalue of a matrix, respectively. From (70) it is clear that $V(t)$ is a non-negative function and bounded by the following inequalities

$$\bar{\lambda}_1 \|\bar{x}\|^2 \leq V(\bar{x}) \leq \bar{\lambda}_2 \|\bar{x}\|^2 \tag{73}$$

where $\bar{\lambda}_1$, $\bar{\lambda}_2 \in \mathbb{R}$ are positive bounding constants defined as follows, provided that ε is selected according to (72)

$$\begin{aligned} \bar{\lambda}_1 &\triangleq \frac{1}{2}\min\{\lambda_{\min}\{M_T\}, \lambda_{\min}\{K_T\}\} \\ &\quad -2\varepsilon\lambda_{\max}\{M_T\} \\ \bar{\lambda}_2 &\triangleq \frac{1}{2}\max\{\lambda_{\max}\{M_T\}, \lambda_{\max}\{K_T\}\} \\ &\quad +2\varepsilon\lambda_{\max}\{M_T\}. \end{aligned} \tag{74}$$

To facilitate the subsequent analysis, the time derivative of (68) can be determined as follows

$$\begin{aligned} \dot{V} &= \eta_d^T M_T \dot{\eta}_d + \lambda_d^T K_T \dot{\lambda}_d \\ &\quad +2\varepsilon\dot{\eta}_d^T M_T \lambda_d + 2\varepsilon\eta_d^T M_T \dot{\lambda}_d. \end{aligned} \tag{75}$$

After utilizing (21) and the fact that $\eta_d(t) = \dot{\lambda}_d(t)$, the expression in (75) can be written as

$$\begin{aligned} \dot{V} &= \eta_d^T F - \eta_d^T B_T \eta_d + 2\varepsilon\lambda_d^T F - 2\varepsilon\lambda_d^T B_T \eta_d \\ &\quad -2\varepsilon\lambda_d^T K_T \lambda_d + 2\varepsilon\eta_d^T M_T \eta_d. \end{aligned} \tag{76}$$

The right-hand side of (76) can be upper bounded as follows

$$\begin{aligned} \dot{V} &\leq \frac{1}{\delta_1}\|\eta_d\|^2 + \delta_1\|F\|^2 - \lambda_{\min}\{B_T\}\|\eta_d\|^2 \\ &\quad +2\varepsilon\left[\delta_2\|\lambda_d\|^2 + \frac{1}{\delta_2}\|F\|^2\right] \\ &\quad +2\varepsilon\lambda_{\max}\{B_T\}\left[\delta_3\|\lambda_d\|^2 + \frac{1}{\delta_3}\|\eta_d\|^2\right] \\ &\quad -2\varepsilon\lambda_{\min}\{K_T\}\|\lambda_d\|^2 + 2\varepsilon\lambda_{\max}\{M_T\}\|\eta_d\|^2 \end{aligned} \tag{77}$$

where the following properties were utilized

$$\begin{aligned} \eta_d^T F &\leq \frac{1}{\delta_1}\|\eta_d\|^2 + \delta_1\|F\|^2 \\ -\eta_d^T B_T \eta_d &\leq -\lambda_{\min}\{B_T\}\|\eta_d\|^2 \\ \lambda_d^T F &\leq \delta_2\|\lambda_d\|^2 + \frac{1}{\delta_2}\|F\|^2 \\ -\lambda_d^T B_T \eta_d &\leq \lambda_{\max}\{B_T\}\left[\delta_3\|\lambda_d\|^2 + \frac{1}{\delta_3}\|\eta_d\|^2\right] \\ -\lambda_d^T K_T \lambda_d &\leq -\lambda_{\min}\{K_T\}\|\lambda_d\|^2 \\ \eta_d^T M_T \eta_d &\leq \lambda_{\max}\{M_T\}\|\eta_d\|^2 \end{aligned}$$

where $\delta_1, \delta_2, \delta_3 \in \mathbb{R}$ are positive bounding constants.

The expression in (77) can be rearranged as follows

$$\begin{aligned} \dot{V} &\leq -\left(\lambda_{\min}\{B_T\} - \frac{1}{\delta_1} - \frac{2\varepsilon\lambda_{\max}\{B_T\}}{\delta_3}\right. \\ &\quad \left. -2\varepsilon\lambda_{\max}\{M_T\}\right)\|\eta_d\|^2 \\ &\quad -2\varepsilon\left(\lambda_{\min}\{K_T\} - \delta_3\lambda_{\max}\{B_T\} - \delta_2\right)\|\lambda_d\|^2 \\ &\quad +\left(\delta_1 + \frac{2\varepsilon}{\delta_2}\right)\|F\|^2. \end{aligned} \tag{78}$$

Provided that ε is selected to satisfy (72) and δ_1, δ_2, δ_3, M_T, B_T, K_T are selected to satisfy the following sufficient conditions

$$\begin{aligned} \lambda_{\min}\{B_T\} &> \frac{1}{\delta_1} + \frac{2\varepsilon\lambda_{\max}\{B_T\}}{\delta_3} \\ &\quad +2\varepsilon\lambda_{\max}\{M_T\} \end{aligned} \tag{79}$$

$$\lambda_{\min}\{K_T\} > \delta_3\lambda_{\max}\{B_T\} + \delta_2 \tag{80}$$

along with the Assumption 1, then the right-hand side of (78) can be upper bounded as follows

$$\dot{V} \leq -\frac{\min\{\gamma_a, \gamma_b\}}{\bar{\lambda}_2}V + \epsilon \tag{81}$$

where (71) and (73) were utilized, and γ_a, γ_b, $\epsilon \in \mathbb{R}$ denote positive bounding constants.

From (68) - (70), and (73), and the fact that $\mathrm{F}(t) \in \mathcal{L}_\infty$, the expression in (81) can be used with the result from [7] to prove that $\bar{x}(t)$, $\lambda_d(t)$, $\eta_d(t) \in \mathcal{L}_\infty$. By utilizing the fact that $\eta_d(t) \in \mathcal{L}_\infty$ along with (20) and Remark 2, it is clear that $\xi_d(t)$, $\dot{\xi}_d(t)$, $\varphi\left(\xi_p(t)\right) \in \mathcal{L}_\infty$. Based on (21), and the fact that $F(t) \in \mathcal{L}_\infty$ then $\dot{\eta}_d(t) \in \mathcal{L}_\infty$.

After utilizing the above boundedness statements along with Remark 2 and the first time derivative of (20), it is clear that $\ddot{\xi}_d(t) \in \mathcal{L}_\infty$. The time derivative of (21) can be written as follows

$$M_T \ddot{\eta}_d + B_T \dot{\eta}_d + K_T \eta_d = \dot{F} \tag{82}$$

where the fact $\eta_d(t) = \dot{\lambda}_d(t)$ was utilized. After utilizing the fact that $\eta_d(t)$, $\dot{\eta}_d(t) \in \mathcal{L}_\infty$, and the assumption that $\dot{F}_H(t)$, $\dot{F}_E(t) \in \mathcal{L}_\infty$ along with (82), it is clear that $\ddot{\eta}_d(t) \in \mathcal{L}_\infty$. The second time derivative of (20) can be written as follows

$$\dddot{\xi}_d \triangleq \gamma \frac{d^2}{dt^2} \left(\begin{bmatrix} \varphi^T(\xi_p) & 0_r^T \end{bmatrix}^T \right) + \dddot{\eta}_d. \tag{83}$$

After utilizing the above boundedness statements and Remark 2 along with (83), then $\dddot{\xi}_d(t) \in \mathcal{L}_\infty$. The time derivative of (82) can be written as follows

$$M_T \dddot{\eta}_d + B_T \ddot{\eta}_d + K_T \dot{\eta}_d = \ddot{F} \tag{84}$$

After utilizing the fact that $\dot{\eta}_d(t)$, $\ddot{\eta}_d(t) \in \mathcal{L}_\infty$ and the assumption that $\ddot{F}_H(t)$, $\ddot{F}_E(t) \in \mathcal{L}_\infty$, from (84) it can be showed that $\dddot{\eta}_d(t) \in \mathcal{L}_\infty$. After taking time derivative of (83) and utilizing the facts that $\xi_d(t)$, $\dot{\xi}_d(t)$, $\ddot{\xi}_d(t)$, $\dddot{\xi}_d(t)$, $\ddddot{\eta}_d(t) \in \mathcal{L}_\infty$, then it is clear that $\ddddot{\xi}_d(t) \in \mathcal{L}_\infty$. By utilizing the above boundedness statements along with (19), it is clear that $x_d(t)$, $\dot{x}_d(t)$, $\ddot{x}_d(t)$, $\dddot{x}_d(t)$, and $\ddddot{x}_d(t) \in \mathcal{L}_\infty$.

B Proof of Theorem 1

Lemma 1 *Let the auxiliary functions $L_1(t)$, $L_2(t) \in \mathbb{R}$ be defined as follows*

$$\begin{aligned} L_1 &\triangleq r^T (N_d - \beta_1 sgn(e_2)) \\ L_2 &\triangleq -\beta_2 \dot{e}_2^T sgn(e_2) \end{aligned} \tag{85}$$

where β_1 and β_2 were introduced in (34). Provided that β_1 is selected to satisfy the following sufficient condition

$$\beta_1 > \varsigma_1 + \frac{1}{\alpha_1}\varsigma_2 \tag{86}$$

where ς_1 and ς_2 were introduced in (33), and α_1 was introduced in (15), then

$$\int_{t_0}^{t} L_1(\tau)\, d\tau \leq \xi_{b1} \qquad \int_{t_0}^{t} L_2(\tau)\, d\tau \leq \xi_{b2} \tag{87}$$

where ξ_{b1}, $\xi_{b2} \in \mathbb{R}$ are positive constants defined as

$$\begin{aligned} \xi_{b1} &\triangleq \beta_1 \sum_{i=1}^{2n} |e_{2i}(t_0)| - e_2^T(t_0) N_d(t_0) \\ \xi_{b2} &\triangleq \beta_2 \sum_{i=1}^{2n} |e_{2i}(t_0)|. \end{aligned} \tag{88}$$

Proof. After substituting (15) into $L_1(t)$ defined in (85) and then integrating in time, results in the following expression

$$\begin{aligned} \int_{t_0}^{t} L_1(\tau)\, d\tau &= \alpha_1 \int_{t_0}^{t} e_2^T(\tau) [N_d(\tau) - \beta_1 sgn(e_2(\tau))]\, d\tau \\ &\quad + \int_{t_0}^{t} \frac{de_2^T(\tau)}{d\tau} N_d(\tau)\, d\tau \\ &\quad - \beta_1 \int_{t_0}^{t} \frac{de_2^T(\tau)}{d\tau} sgn(e_2(\tau))\, d\tau. \end{aligned} \tag{89}$$

After integrating the second integral on the right side of (89) by parts and evaluating the last integral, the following expression is obtained

$$\begin{aligned} \int_{t_0}^{t} L_1(\tau)\, d\tau &= \alpha_1 \int_{t_0}^{t} e_2^T \left(N_d - \frac{1}{\alpha_1}\frac{dN_d}{d\tau} \right. \\ &\quad \left. - \beta_1 sgn(e_2) \right) d\tau + e_2^T(t) N_d(t) \\ &\quad - \beta_1 \sum_{i=1}^{2n} |e_{2i}(t)| + \xi_{b1}. \end{aligned} \tag{90}$$

The right-hand side of (90) can be upper bounded as follows

$$\begin{aligned} \int_{t_0}^{t} L_1(\tau)\, d\tau &\leqslant \alpha_1 \int_{t_0}^{t} \sum_{i=1}^{2n} |e_{2i}(\tau)| \left(|N_{d_i}(\tau)| \right. \\ &\quad \left. + \frac{1}{\alpha_1} \left| \frac{dN_{d_i}(\tau)}{d\tau} \right| - \beta_1 \right) d\tau \\ &\quad + \sum_{i=1}^{2n} |e_{2i}(t)| \left(|N_{d_i}(t)| - \beta_1 \right) + \xi_{b1}. \end{aligned} \tag{91}$$

If β_1 is chosen according to (39), then the first inequality in (87) can be proven from (91). The second inequality in (87) can be obtained by integrating the expression for $L_2(t)$ defined in (85) as follows

$$\begin{aligned} \int_{t_0}^{t} L_2(\tau)\, d\sigma &= -\beta_2 \int_{t_0}^{t} \dot{e}_2^T(\tau) sgn(e_2(\tau))\, d\tau \\ &= \xi_{b2} - \beta_2 \sum_{i=1}^{2n} |e_{2i}(t)| \leq \xi_{b2}. \blacksquare \end{aligned} \tag{92}$$

The following is the proof of Theorem 1.

Proof. Let the auxiliary functions $P_1(t)$, $P_2(t) \in \mathbb{R}$ be defined as follows

$$P_1 \triangleq \xi_{b1} - \int_{t_0}^{t} L_1(\tau)\, d\tau \geq 0 \tag{93}$$

$$P_2 \triangleq \xi_{b2} - \int_{t_0}^{t} L_2(\tau)\, d\tau \geq 0 \tag{94}$$

where $L_1(t)$, $L_2(t)$, ξ_{b1} and ξ_{b2} were defined in Lemma 1. The proof of Lemma 1 ensures that $P_1(t)$ and $P_2(t)$

are non-negative. Let $V(y,t) \in \mathbb{R}$ denote the following non-negative function

$$V \triangleq \frac{1}{2}e_1^T e_1 + \frac{1}{2}e_2^T e_2 + \frac{1}{2}r^T \bar{M} r + P_1 + P_2 \tag{95}$$

where $y(t) \in \mathbb{R}^{6n+2}$ is defined as follows

$$y \triangleq \begin{bmatrix} z^T & \sqrt{P_1} & \sqrt{P_2} \end{bmatrix}^T \tag{96}$$

where $z(t) \in \mathbb{R}^{6n}$ is defined as follows

$$z \triangleq \begin{bmatrix} e_1^T & e_2^T & r^T \end{bmatrix}^T. \tag{97}$$

Because $\bar{M}(x)$ is assumed to be bounded as defined in (14), (95) is bounded as follows

$$W_1(y) \leq V(y,t) \leq W_2(y) \tag{98}$$

where $W_1(y)$, $W_2(y) \in \mathbb{R}$ are defined as

$$W_1(y) \triangleq \lambda_1 \|y(t)\|^2 \quad W_2(y) \triangleq \lambda_2 \|y(t)\|^2 \tag{99}$$

where $\lambda_1 \triangleq \frac{1}{2}\min\{1, \bar{m}_1\}$ and $\lambda_2 \triangleq \max\{1, \frac{1}{2}\bar{m}_2\}$.

After differentiating (95) in time, the following expression can be obtained

$$\begin{aligned} \dot{V} &= -\alpha_2 e_1^T e_1 - \alpha_1 e_2^T e_2 - r^T (k_s + 1) r \\ &\quad + e_1^T e_2 + r^T \tilde{N} - r^T \beta_2 sgn(e_2) + \beta_2 \dot{e}_2^T sgn(e_2) \end{aligned} \tag{100}$$

where (15), (16), (36), (93), and (94) were utilized. To facilitate the subsequent analysis, the following inequality can be developed from (30) - (32) (see Appendix H)

$$\left\| \tilde{N}(\cdot) \right\| \leq \rho(\|z\|) \|z\| \tag{101}$$

where $\rho(\cdot)$ is a positive, invertible bounding function that is non-decreasing in $\|z\|$. By utilizing (15), (101), and the triangle inequality, $\dot{V}(t)$ can be upper bounded as follows

$$\begin{aligned} \dot{V} &\leq -\alpha_2 e_1^T e_1 - \alpha_1 e_2^T e_2 - r^T (k_s + 1) r \\ &\quad + e_1^T e_1 + e_2^T e_2 + \rho(\|z\|) \|r\| \|z\| \\ &\quad - \alpha_1 e_2^T \beta_2 sgn(e_2). \end{aligned} \tag{102}$$

After utilizing (97), the right-hand side of (102) can be rearranged as follows

$$\begin{aligned} \dot{V} &\leq -\lambda_3 \|z\|^2 + \left[\rho(\|z\|) \|r\| \|z\| - k_s \|r\|^2 \right] \\ &\quad - \alpha_1 \beta_2 \sum_{i=1}^{2n} |e_{2i}| \end{aligned} \tag{103}$$

where $\lambda_3 \triangleq \min\{\alpha_1 - 1, \alpha_2 - 1, 1\}$. Completing the squares on the bracketed term in (103), yields the following expression

$$\dot{V} \leq -\left(\lambda_3 - \frac{\rho^2(\|z\|)}{4k_s} \right) \|z\|^2 - \alpha_1 \beta_2 \sum_{i=1}^{2n} |e_{2i}|. \tag{104}$$

Provided α_1 and α_2 are selected to be greater than 2 and k_s is selected according to the following sufficient condition

$$k_s \geq \frac{\rho^2(\|z\|)}{4\lambda_3} \text{ or } \|z\| \leq \rho^{-1}\left(2\sqrt{k_s \lambda_3}\right) \tag{105}$$

then based on (104) the following inequality can be developed

$$\dot{V} \leq W(y) - \alpha_1 \beta_2 \sum_{i=1}^{2n} |e_{2i}| \tag{106}$$

where $W(y) \in \mathbb{R}$ denotes the following non-positive function

$$W(y) \triangleq -\beta_0 \|z\|^2 \tag{107}$$

where $\beta_0 \in \mathbb{R}$ is a positive constant. From (95)-(99) and (104)-(107) the regions D and S can be defined as follows

$$\mathcal{D} \triangleq \left\{ y \in \mathbb{R}^{6n+2} \mid \|y\| < \rho^{-1}\left(2\sqrt{k_s \lambda_3}\right) \right\} \tag{108}$$

$$\mathcal{S} \triangleq \left\{ y \in \mathcal{D} \mid W_2(y) < \lambda_1 \left(\rho^{-1}\left(2\sqrt{k_s \lambda_3}\right) \right)^2 \right\}. \tag{109}$$

Note that the region of attraction in (109) can be made arbitrarily large to include any initial conditions by increasing the control gain k_s (i.e., a semi-global stability result). Specifically, (99) and (109) can be used to calculate the region of attraction as follows

$$\begin{aligned} W_2(y(t_0)) &< \lambda_1 \left(\rho^{-1}\left(2\sqrt{k_s \lambda_3}\right) \right)^2 \\ &\implies \|y(t_0)\| < \sqrt{\frac{\lambda_1}{\lambda_2}} \rho^{-1}\left(2\sqrt{k_s \lambda_3}\right), \end{aligned} \tag{110}$$

which can be rearranged as

$$k_s \geq \frac{1}{4\lambda_3} \rho^2 \left(\sqrt{\frac{\lambda_2}{\lambda_1}} \|y(t_0)\| \right). \tag{111}$$

By utilizing (88), (96) and (97) the following explicit expression for $\|y(t_0)\|$ can be derived as follows

$$\begin{aligned} \|y(t_0)\|^2 &= \|e_1(t_0)\|^2 + \|e_2(t_0)\|^2 \\ &\quad + \|r(t_0)\|^2 + \xi_{b1} + \xi_{b2}. \end{aligned} \tag{112}$$

From (95), (106), (109)-(111), it is clear that $V(y,t) \in \mathcal{L}_\infty$ $\forall y(t_0) \in \mathcal{S}$; hence $e_1(t)$, $e_2(t)$, $r(t)$, $z(t)$, $y(t) \in \mathcal{L}_\infty$ $\forall y(t_0) \in \mathcal{S}$. From (106), it is easy to show that $e_2(t) \in \mathcal{L}_1$ $\forall y(t_0) \in \mathcal{S}$. The fact that $e_2(t) \in \mathcal{L}_1$ $\forall y(t_0) \in \mathcal{S}$ can be used along with (16) to determine that $e_1(t), \dot{e}_1(t) \in \mathcal{L}_1$ $\forall y(t_0) \in \mathcal{S}$. From (7), (17) and the fact that $x_d(t) \in \mathcal{L}_\infty$, it is clear that $x(t)$, $x_m(t)$, $x_s(t) \in \mathcal{L}_\infty$ $\forall y(t_0) \in \mathcal{S}$. From (15) and (16) it is also clear that $\dot{e}_2(t)$, $\dot{e}_1(t) \in \mathcal{L}_\infty$ $\forall y(t_0) \in \mathcal{S}$. Using these boundedness statements, from

(35) it is clear that $\dot{\bar{u}}(t) \in \mathcal{L}_\infty \ \forall y(t_0) \in \mathcal{S}$. Since $\ddot{e}_1(t) \in \mathcal{L}_\infty$, from the second time derivative of (17), and the fact that $\ddot{x}_d(t) \in \mathcal{L}_\infty$ along with (27), it is clear that $\bar{u}(t) \in \mathcal{L}_\infty \ \forall y(t_0) \in \mathcal{S}$. The previous boundedness statements can be used along with (36), (101), and Remark 4 to prove that $\dot{r}(t) \in \mathcal{L}_\infty \ \forall y(t_0) \in \mathcal{S}$. These bounding statements can be used along with the time derivative of (107) to prove that $\dot{W}(y(t)) \in \mathcal{L}_\infty \ \forall y(t_0) \in S$; hence, $W(y(t))$ is uniformly continuous. Standard signal chasing arguments can be used to prove that all remaining signals are bounded. A direct application of Theorem 8.4 in [13] can be used to prove that $\|z(t)\| \to 0$ as $t \to \infty$ $\forall y(t_0) \in \mathcal{S}$. From (97), it is clear that $\|r(t)\| \to 0$ as $t \to \infty \ \forall y(t_0) \in \mathcal{S}$. Based on the definitions given in (15) and (16), standard linear analysis tools can be used to prove that if $\|r(t)\| \to 0$ then $\|\dot{e}_2(t)\|$, $\|e_2(t)\|$, $\|\dot{e}_1(t)\|$, $\|e_1(t)\| \to 0$ as $t \to \infty \ \forall y(t_0) \in \mathcal{S}$. Based on the definition of $x(t)$ in (7) and $e_1(t)$ in (17), it is clear that if $\|e_1(t)\| \to 0$ then $x_s(t) \to x_m(t)$ and $x_m(t) \to \xi_d(t)$.

C Proof of Theorem 2

Proof. Since the user assist mechanism is disabled (i.e., $\gamma = 0$), the target system defined in (20) and (21) can be simplified to (25). Let $V_p(t) \in \mathbb{R}$ denote the following non-negative function

$$V_p \triangleq \frac{1}{2}\dot{\xi}_d^T M_T \dot{\xi}_d + \frac{1}{2}\xi_d^T K_T \xi_d. \tag{113}$$

After differentiating (113) in time, the following simplified expression can be obtained

$$\dot{V}_p = \dot{\xi}_d^T F - \dot{\xi}_d^T B_T \dot{\xi}_d \tag{114}$$

where (25) was utilized. Based on the fact that B_T is a constant positive definite, diagonal matrix, the following inequality can be obtained

$$\dot{V}_p \leq \dot{\xi}_d^T F. \tag{115}$$

Integrating both sides of (115), results in the following inequality

$$-c_2 \leq V_p(t) - V_p(t_0) \leq \int_{t_0}^{t} \dot{\xi}_d^T(\sigma) F(\sigma) d\sigma \tag{116}$$

where $c_2 \in \mathbb{R}$ is a positive bounded constant (since $V_p(t)$ is bounded from the trajectory generation system in (25)).

By using the transformation in (7), the left-hand side of (6) can be expressed as

$$\begin{aligned} &\int_{t_0}^{t} \begin{bmatrix} \dot{x}_m^T(\tau) & \dot{x}_s^T(\tau) \end{bmatrix} \begin{bmatrix} F_H(\tau) \\ F_E(\tau) \end{bmatrix} d\tau \\ &= \int_{t_0}^{t} \dot{x}^T \bar{F} d\tau. \end{aligned} \tag{117}$$

By substituting the time derivative of (17) into (117), the following expression can be obtained

$$\begin{aligned} \int_{t_0}^{t} \dot{x}^T(\tau) \bar{F}(\tau) d\tau &= \int_{t_0}^{t} \dot{\xi}_d^T(\tau) F(\tau) d\tau \\ &\quad - \int_{t_0}^{t} \dot{e}_1^T(\tau) \bar{F}(\tau) d\tau \end{aligned} \tag{118}$$

where (13),(19) and (22) were utilized. Based on (116), it is clear that $\int_{t_0}^{t} \dot{\xi}_d^T(\tau) F(\tau) d\tau$ is lower bounded by $-c_2$. The fact that $\dot{e}_1(t) \in \mathcal{L}_1$ (see the proof for Theorem 1) and the assumption that $\bar{F}(t) \in \mathcal{L}_\infty$ can be used to show that the second integral of (118) is bounded. Hence, these facts can be applied to (117) and (118) to prove that

$$\int_{t_0}^{t} \begin{bmatrix} \dot{x}_m^T(\tau) & \dot{x}_s^T(\tau) \end{bmatrix} \begin{bmatrix} F_H(\tau) \\ F_E(\tau) \end{bmatrix} d\tau \geq -c_3^2 \tag{119}$$

where $c_3 \in \mathbb{R}$ is a bounded constant. ■

D Proof of Theorem 3

Lemma 2 *Let the auxiliary functions $L_1(t)$, $L_2(t) \in \mathbb{R}$ be defined as follows*

$$\begin{aligned} L_1 &\triangleq -r^T\left(\dot{\bar{F}} + \beta_1 sgn(e_2)\right) \\ L_2 &\triangleq -\beta_2 \dot{e}_2^T sgn(e_2) \end{aligned} \tag{120}$$

where β_1 and β_2 were introduced in (61). Provided that β_1 is selected to satisfy the following sufficient condition

$$\beta_1 > \varsigma_3 + \varsigma_4, \tag{121}$$

where ς_3 and ς_4 were introduced in (64), then

$$\int_{t_0}^{t} L_1(\tau) d\tau \leq \xi_{b1} \qquad \int_{t_0}^{t} L_2(\tau) d\tau \leq \xi_{b2} \tag{122}$$

where ξ_{b1}, $\xi_{b2} \in \mathbb{R}$ are positive constants defined as

$$\begin{aligned} \xi_{b1} &\triangleq \beta_1 \sum_{i=1}^{2n} |e_{2i}(t_0)| - e_2^T(t_0)\left(-\dot{\bar{F}}(t_0)\right) \\ \xi_{b2} &\triangleq \beta_2 \sum_{i=1}^{2n} |e_{2i}(t_0)|. \end{aligned} \tag{123}$$

Proof. After substituting (44) into $L_1(t)$ defined in (120) and then integrating in time, results in the following expression

$$\begin{aligned} \int_{t_0}^{t} L_1(\tau) d\tau &= \int_{t_0}^{t} e_2^T(\tau)\left[-\dot{\bar{F}}(\tau) - \beta_1 sgn(e_2(\tau))\right] d\tau \\ &\quad + \int_{t_0}^{t} \frac{de_2^T(\tau)}{d\tau}\left(-\dot{\bar{F}}(\tau)\right) d\tau \\ &\quad - \beta_1 \int_{t_0}^{t} \frac{de_2^T(\tau)}{d\tau} sgn(e_2(\tau)) d\tau. \end{aligned} \tag{124}$$

After integrating the second integral on the right-hand side of (124) by parts and evaluating the last integral, the following expression is obtained

$$\begin{aligned}\int_{t_0}^{t} L_1(\tau)\,d\tau &= \int_{t_0}^{t} e_2^T(\tau)\Big(-\dot{\bar{F}}(\tau)+\ddot{\bar{F}}(\tau) \\ &\quad -\beta_1 sgn(e_2(\tau))\Big)\,d\tau \qquad (125)\\ &\quad -e_2^T(t)\,\dot{\bar{F}}(t)-\beta_1\sum_{i=1}^{2n}|e_{2i}(t)|+\xi_{b1}.\end{aligned}$$

The right-hand side of (125) can be upper bounded as follows

$$\begin{aligned}\int_{t_0}^{t} L_1(\tau)\,d\tau &\leqslant \int_{t_0}^{t}\sum_{i=1}^{2n}|e_{2i}(\tau)|\left(\left|\dot{\bar{F}}_i(\tau)\right|\right. \qquad (126)\\ &\quad \left.+\left|\ddot{\bar{F}}_i(\tau)\right|-\beta_1\right)d\tau \\ &\quad +\sum_{i=1}^{2n}|e_{2i}(t)|\left(\left|\dot{\bar{F}}_i(t)\right|-\beta_1\right)+\xi_{b1}.\end{aligned}$$

If β_1 is chosen to satisfy (121), then the first inequality in (122) can be proven from (126). The second inequality in (122) can be obtained by integrating $L_2(t)$, defined in (120) as follows

$$\begin{aligned}\int_{t_0}^{t} L_2(\tau)\,d\sigma &= -\beta_2\int_{t_0}^{t}\dot{e}_2^T(\tau)\,sgn(e_2(\tau))\,d\tau \\ &= \xi_{b2}-\beta_2\sum_{i=1}^{2n}|e_{2i}(t)|\leq\xi_{b2}. \qquad (127)\end{aligned}$$

The following is the proof of Theorem 3.

Proof. Let the auxiliary functions $P_1(t)$, $P_2(t)\in\mathbb{R}$ be defined as follows

$$P_1 \triangleq \xi_{b1}-\int_{t_0}^{t} L_1(\tau)\,d\tau \geq 0 \qquad (128)$$

$$P_2 \triangleq \xi_{b2}-\int_{t_0}^{t} L_2(\tau)\,d\tau \geq 0 \qquad (129)$$

where $L_1(t)$, $L_2(t)$, ξ_{b1} and ξ_{b2} were defined in Lemma 2. The proof of Lemma 2 ensures that $P_1(t)$ and $P_2(t)$ are non-negative. Let $V_1(y,t)\in\mathbb{R}$ denote the following non-negative function

$$V_1 \triangleq \frac{1}{2}e_2^T e_2+\frac{1}{2}r^T r+P_1+P_2 \qquad (130)$$

where $y(t)\in\mathbb{R}^{4n+2}$ is defined as

$$y \triangleq \left[\begin{array}{cccc} e_2^T & r^T & \sqrt{P_1} & \sqrt{P_2}\end{array}\right]^T. \qquad (131)$$

Note that (130) is bounded by the following inequalities

$$W_3(y)\leq V_1(y,t)\leq W_4(y) \qquad (132)$$

where $W_3(y)$, $W_4(y)\in\mathbb{R}$ are defined as

$$W_3(y)=\lambda_4\|y(t)\|^2 \qquad W_4(y)=\lambda_5\|y(t)\|^2 \qquad (133)$$

where λ_4, $\lambda_5\in\mathbb{R}$ are positive bounding constants.

After differentiating (130) in time, results in the following expression

$$\dot{V}_1=-e_2^T e_2-k_s r^T r-\beta_2 e_2^T sgn(e_2) \qquad (134)$$

where (44), (63), (128), and (129) were utilized. The expression in (134) can be rewritten as

$$\dot{V}_1=-\|e_2\|^2-k_s\|r\|^2-\beta_2\sum_{i=1}^{2n}|e_{2i}|. \qquad (135)$$

From (130) and (135), it is clear that $V_1(y,t)\in\mathcal{L}_\infty$; hence, $e_2(t)\in\mathcal{L}_\infty\cap\mathcal{L}_2\cap\mathcal{L}_1$, $r(t)\in\mathcal{L}_\infty\cap\mathcal{L}_2$, and $y(t)\in\mathcal{L}_\infty$. Since $e_2(t)$, $r(t)\in\mathcal{L}_\infty$, then (44) and (62) can be used to prove that $\dot{e}_2(t)$, $\dot{\hat{F}}(t)\in\mathcal{L}_\infty$. Given that $e_2(t), r(t)$, $\dot{\hat{F}}(t)\in\mathcal{L}_\infty$ and the assumption that $\dot{\bar{F}}(t)\in\mathcal{L}_\infty$, (60) can be used to prove that $\dot{r}(t)\in\mathcal{L}_\infty$. Barbalat's Lemma can be utilized to prove

$$\|e_2(t)\|, \|r(t)\|\to 0 \quad as \quad t\to\infty. \qquad (136)$$

From (44), (45), (136) and the fact that $\bar{M}(x)\in\mathcal{L}_\infty$, standard linear analysis arguments can be used to prove that $e_1(t)$, $\dot{e}_1(t)$, $\dot{e}_2(t)\in\mathcal{L}_\infty$ and $e_1(t)$, $\dot{e}_1(t)\in\mathcal{L}_1$, and that

$$\|e_1(t)\|, \|\dot{e}_1(t)\|, \|\dot{e}_2(t)\|\to 0 \quad as \quad t\to\infty. \qquad (137)$$

By using the assumption that $\bar{F}(t)\in\mathcal{L}_\infty$ and the fact that $\dot{e}_2(t)\in\mathcal{L}_\infty$ from (58) it is clear that $\hat{F}(t)\in\mathcal{L}_\infty$. Since $\hat{F}(t)\in\mathcal{L}_\infty$, (49) and the proof in Appendix F can be used to prove that $\lambda_d(t)$, $\eta_d(t)$, $\dot{\eta}_d(t)$, $\xi_d(t)$, $\dot{\xi}_d(t)$, $\ddot{\xi}_d(t)\in\mathcal{L}_\infty$. Using these facts along with (42), (46) and their first time derivatives, it is clear that $x(t)$, $\dot{x}(t)$, $x_m(t)$, $\dot{x}_m(t)$, $x_s(t)$, $\dot{x}_s(t)\in\mathcal{L}_\infty$. Since $e_1(t)$, $\dot{e}_1(t)$, $\bar{M}(x)$, $\dot{\bar{M}}(x)\in\mathcal{L}_\infty$, it is clear from (57) that $\bar{T}_1(t)\in\mathcal{L}_\infty$, and using previously stated bounding properties, $\bar{T}(t)\in\mathcal{L}_\infty$. It is also possible to state that $\bar{T}_1(t)\in\mathcal{L}_1$, where (57) was utilized. Based on the definition of $x(t)$ in (42) and the previously stated bounding properties, it is clear that $x_s(t)\to x_m(t)$ and $x_m(t)\to\xi_1(t)$. From these bounding statements and standard signal chasing arguments, all signals can be shown to be bounded. ■

E Proof of Theorem 4

Proof. Since the user assist mechanism is disabled (i.e., $\gamma=0$), the target system defined in (48) and (49) can be simplified to (52). To assist in the subsequent analysis,

the following expression can be developed from integration by parts

$$\int_{t_0}^{t} \bar{M}\ddot{e}_1(\tau)\,d\tau = \bar{M}\dot{e}_1(t) - \bar{M}\dot{e}_1(t_0) - \int_{t_0}^{t} \dot{\bar{M}}\,\dot{e}_1(\tau)\,d\tau. \quad (138)$$

Since $\bar{M}(x)$, $\dot{\bar{M}}(x)$, $\dot{e}_1(t) \in \mathcal{L}_\infty$, and $\dot{e}_1(t) \in \mathcal{L}_1$, then $\int_{t_0}^{t} \bar{M}\ddot{e}_1(\tau)\,d\tau \in \mathcal{L}_\infty$. After integrating (55) as follows

$$\int_{t_0}^{t} \tilde{F}(\tau)\,d\tau = -\int_{t_0}^{t} \bar{M}\ddot{e}_1(\tau)\,d\tau - \int_{t_0}^{t} \bar{T}_1(\tau)\,d\tau \quad (139)$$

and using the facts that $\bar{T}_1(t) \in \mathcal{L}_1$ (see proof of Theorem 3) and that $\int_{t_0}^{t} \bar{M}\ddot{e}_1(\tau)\,d\tau \in \mathcal{L}_\infty$, it is clear that $\tilde{F}(t) \in \mathcal{L}_1$, where $\tilde{F}(t) \in \mathbb{R}^{2n}$ is defined as follows

$$\tilde{F} \triangleq \bar{F} - \hat{F}. \quad (140)$$

The expression in (140) can be decomposed as $\tilde{F}(t) = \begin{bmatrix} \tilde{F}_1^T & \tilde{F}_2^T \end{bmatrix}^T$, where $\tilde{F}_1(t), \tilde{F}_2(t) \in \mathbb{R}^n$. After utilizing the fact that $\hat{F}(t_0) = 0_{2n}$, the following can be derived

$$\hat{F}(t) = \int_{t_0}^{t} \dot{\hat{F}}(\tau)\,d\tau. \quad (141)$$

From the proof of Theorem 3 (see Appendix D), it is clear that $\hat{F}(t) \in L_\infty$, then from (141) it is also clear that $\dot{\hat{F}}(t) \in \mathcal{L}_1$.

By using the transformation in (42), the passivity objective in (6) can be rewritten as follows

$$\int_{t_0}^{t} \begin{bmatrix} \dot{x}_m^T(\tau) & \dot{x}_s^T(\tau) \end{bmatrix} \begin{bmatrix} F_H(\tau) \\ F_E(\tau) \end{bmatrix} d\tau \quad (142)$$
$$= \int_{t_0}^{t} \dot{x}^T \bar{F} d\tau - \int_{t_0}^{t} \begin{bmatrix} 0_n^T & \dot{\xi}_2^T \end{bmatrix} \bar{F} d\tau.$$

By utilizing (140) and the time derivative of (46), (142) can be rewritten as follows

$$\int_{t_0}^{t} \dot{x}^T \bar{F} d\tau - \int_{t_0}^{t} \begin{bmatrix} 0_n^T & \dot{\xi}_2^T \end{bmatrix} \bar{F} d\tau \quad (143)$$
$$= \int_{t_0}^{t} \dot{\xi}_1^T(\tau)\tilde{F}_1(\tau)\,d\tau + \int_{t_0}^{t} \dot{\xi}_1^T(\tau)\hat{F}_1(\tau)\,d\tau - \int_{t_0}^{t} \dot{e}_1^T(\tau)\bar{F}(\tau)\,d\tau.$$

Following expression can be developed from integration by parts of the second integral at the right-hand side of (143)

$$\int_{t_0}^{t} \dot{x}^T \bar{F} d\tau - \int_{t_0}^{t} \begin{bmatrix} 0_n^T & \dot{\xi}_2^T \end{bmatrix} \bar{F} d\tau \quad (144)$$
$$= \int_{t_0}^{t} \dot{\xi}_1^T(\tau)\tilde{F}_1(\tau)\,d\tau - \int_{t_0}^{t} \xi_1^T(\tau)\dot{\hat{F}}_1(\tau)\,d\tau + \xi_1^T(t)\hat{F}_1(t) - \int_{t_0}^{t} \dot{e}_1^T(\tau)\bar{F}(\tau)\,d\tau$$

where $\hat{F}(t_0) = 0_{2n}$ is both utilized. Since $\dot{\xi}_1(t) \in \mathcal{L}_\infty$ and $\tilde{F}(t) \in \mathcal{L}_1$, it is clear that the first integral expression in (144) is bounded and a lower negative bound exists. Since $\xi_1(t) \in \mathcal{L}_\infty$ and $\dot{\hat{F}}(t) \in \mathcal{L}_1$ it is clear that the second integral expression in (144) is bounded and a lower negative bound exists, and since $\xi_1(t)$, $\hat{F}(t) \in \mathcal{L}_\infty$ then third expression is also bounded and a lower negative bound exists. Finally, because $\dot{e}_1(t) \in \mathcal{L}_1$ and $\bar{F}(t) \in \mathcal{L}_\infty$, it is possible to show that the last integral in (144) is also bounded and a lower negative bound exists. Hence, these facts can be applied to (142) to prove that

$$\int_{t_0}^{t} \begin{bmatrix} \dot{x}_m^T(\tau) & \dot{x}_s^T(\tau) \end{bmatrix} \begin{bmatrix} F_H(\tau) \\ F_E(\tau) \end{bmatrix} d\tau \geq -c_4^2 \quad (145)$$

where $c_4 \in \mathbb{R}$ is a bounded constant. ■

F UMIF Desired Trajectory Stability Analysis

In the proof of Theorem 3 (see Appendix D), it is proven that $e_1(t)$, $e_2(t)$, $r(t)$, $\hat{F}(t)$, $\dot{\hat{F}}(t) \in \mathcal{L}_\infty$ as well as that $\|e_1(t)\|$, $\|e_2(t)\|$, and $\|r(t)\| \to 0$ as $t \to \infty$ regardless of whether or not $x(t)$, $\xi_d(t)$, $\lambda_d(t)$, $\eta_d(t)$, $\dot{\eta}_d(t) \in \mathcal{L}_\infty$. Therefore the fact that $\hat{F}(t) \in \mathcal{L}_\infty$ can be used in the subsequent analysis. To prove that $\lambda_d(t)$, $\eta_d(t) \in \mathcal{L}_\infty$, let $V(t) \in \mathbb{R}$ denote the following function

$$V \triangleq V_1 + V_2 \quad (146)$$

where $V_1(t) \in \mathbb{R}$ denotes the following non-negative function

$$V_1 \triangleq \frac{1}{2}\eta_d^T M_T \eta_d + \frac{1}{2}\lambda_d^T K_T \lambda_d \quad (147)$$

where $\lambda_d(t)$, $\eta_d(t)$, M_T and K_T were introduced in (49). The expression given in (147) can be lower bounded by the auxiliary function, $V_2(\bar{x}) \in \mathbb{R}$, defined as follows

$$V_2 \triangleq 2\varepsilon\eta_d^T M_T \lambda_d \leq V_1 \quad (148)$$

where $\bar{x}(t) \in \mathbb{R}^{4n}$ is defined as

$$\bar{x} \triangleq \begin{bmatrix} \lambda_d^T & \eta_d^T \end{bmatrix}^T \quad (149)$$

and $\varepsilon \in \mathbb{R}$ is a positive bounding constant selected according to the following inequality

$$\varepsilon < \frac{\min\{\lambda_{\min}\{M_T\}, \lambda_{\min}\{K_T\}\}}{4\lambda_{\max}\{M_T\}} \quad (150)$$

where $\lambda_{\min}\{\cdot\}$ and $\lambda_{\max}\{\cdot\}$ denote the minimum and maximum eigenvalue of a matrix, respectively. From (148) it is clear that $V(t)$ is a non-negative function and bounded by the following inequalities

$$\bar{\lambda}_1 \|\bar{x}\|^2 \leq V(\bar{x}) \leq \bar{\lambda}_2 \|\bar{x}\|^2 \quad (151)$$

where $\bar{\lambda}_1, \bar{\lambda}_2 \in \mathbb{R}$ are positive constants defined as follows, provided that ε is selected according to (150)

$$\begin{aligned} \bar{\lambda}_1 &\triangleq \frac{1}{2}\min\{\lambda_{\min}\{M_T\}, \lambda_{\min}\{K_T\}\} \\ &\quad -2\varepsilon\lambda_{\max}\{M_T\} \\ \bar{\lambda}_2 &\triangleq \frac{1}{2}\max\{\lambda_{\max}\{M_T\}, \lambda_{\max}\{K_T\}\} \\ &\quad +2\varepsilon\lambda_{\max}\{M_T\}. \end{aligned} \tag{152}$$

To facilitate the subsequent analysis, the time derivative of (146) can be determined as follows

$$\begin{aligned} \dot{V} &= \eta_d^T M_T \dot{\eta}_d + \lambda_d^T K_T \dot{\lambda}_d \\ &\quad +2\varepsilon\dot{\eta}_d^T M_T \lambda_d + 2\varepsilon\eta_d^T M_T \dot{\lambda}_d. \end{aligned} \tag{153}$$

After utilizing (49) and the fact that $\eta_d(t) = \dot{\lambda}_d(t)$, the expression in (153) can be written as

$$\begin{aligned} \dot{V} &= \eta_d^T \left(M_T \bar{M}^{-1}\right)\hat{F} - \eta_d^T B_T \eta_d + 2\varepsilon\lambda_d^T M_T \bar{M}^{-1}\hat{F} \\ &\quad -2\varepsilon\lambda_d^T B_T \eta_d - 2\varepsilon\lambda_d^T K_T \lambda_d + 2\varepsilon\eta_d^T M_T \eta_d. \end{aligned} \tag{154}$$

The right-hand side of (154) can be upper bounded as follows

$$\begin{aligned} \dot{V} &\leq \xi_{\bar{m}}\lambda_{\max}\{M_T\}\left[\delta_1\|\eta_d\|^2 + \frac{1}{\delta_1}\left\|\hat{F}\right\|^2\right] \\ &\quad -\lambda_{\min}\{B_T\}\|\eta_d\|^2 \\ &\quad +2\varepsilon\xi_{\bar{m}}\lambda_{\max}\{M_T\}\left[\delta_3\|\lambda_d\|^2 + \frac{1}{\delta_3}\left\|\hat{F}\right\|^2\right] \\ &\quad +2\varepsilon\lambda_{\max}\{B_T\}\left[\delta_2\|\lambda_d\|^2 + \frac{1}{\delta_2}\|\eta_d\|^2\right] \\ &\quad -2\varepsilon\lambda_{\min}\{K_T\}\|\lambda_d\|^2 + 2\varepsilon\lambda_{\max}\{M_T\}\|\eta_d\|^2 \end{aligned} \tag{155}$$

where the following properties were utilized

$$\eta_d^T M_T \bar{M}^{-1}\hat{F} \leq \xi_{\bar{m}}\lambda_{\max}\{M_T\}\left[\delta_1\|\eta_d\|^2 + \frac{1}{\delta_1}\left\|\hat{F}\right\|^2\right] \tag{156}$$

$$-\eta_d^T B_T \eta_d \leq -\lambda_{\min}\{B_T\}\|\eta_d\|^2 \tag{157}$$

$$2\varepsilon\lambda_d^T M_T \bar{M}^{-1}\hat{F} \leq 2\varepsilon\xi_{\bar{m}}\lambda_{\max}\{M_T\}\left[\delta_3\|\lambda_d\|^2 + \frac{1}{\delta_3}\left\|\hat{F}\right\|^2\right] \tag{158}$$

$$-2\varepsilon\lambda_d^T B_T \eta_d \leq 2\varepsilon\lambda_{\max}\{B_T\}\left[\delta_2\|\lambda_d\|^2 + \frac{1}{\delta_2}\|\eta_d\|^2\right] \tag{159}$$

$$-2\varepsilon\lambda_d^T K_T \lambda_d \leq -2\varepsilon\lambda_{\min}\{K_T\}\|\lambda_d\|^2 \tag{160}$$

$$2\varepsilon\eta_d^T M_T \eta_d \leq 2\varepsilon\lambda_{\max}\{M_T\}\|\eta_d\|^2 \tag{161}$$

where $\delta_1, \delta_2, \delta_3 \in \mathbb{R}$ denote positive bounding constants and $\xi_{\bar{m}} \in \mathbb{R}$ denotes positive bounding constant defined as

$$\left\|\bar{M}^{-1}\right\|_\infty \leq \xi_{\bar{m}} \tag{162}$$

where $\left\|\bar{M}^{-1}\right\|_\infty$ denotes the induced infinity norm of the bounded matrix $\bar{M}^{-1}(x)$.

The expression in (155) can be rearranged as follows

$$\begin{aligned} \dot{V} &\leq -\left(\lambda_{\min}\{B_T\} - \xi_{\bar{m}}\delta_1\lambda_{\max}\{M_T\}\right. \\ &\quad \left.-\frac{2\varepsilon\lambda_{\max}\{B_T\}}{\delta_2} - 2\varepsilon\lambda_{\max}\{M_T\}\right)\|\eta_d\|^2 \\ &\quad -2\varepsilon\left(\lambda_{\min}\{K_T\} - \delta_2\lambda_{\max}\{B_T\}\right. \\ &\quad \left.-\xi_{\bar{m}}\delta_3\lambda_{\max}\{M_T\}\right)\|\lambda_d\|^2 \\ &\quad +\xi_{\bar{m}}\lambda_{\max}\{M_T\}\left(\frac{1}{\delta_1} + \frac{2\varepsilon}{\delta_3}\right)\left\|\hat{F}\right\|^2. \end{aligned} \tag{163}$$

Provided δ_1, δ_2, δ_3, M_T, B_T, K_T and ε are selected to satisfy (150) and the following sufficient conditions

$$\begin{aligned} \lambda_{\min}\{B_T\} &> \xi_{\bar{m}}\delta_1\lambda_{\max}\{M_T\} \\ &\quad +\frac{2\varepsilon\lambda_{\max}\{B_T\}}{\delta_2} + 2\varepsilon\lambda_{\max}\{M_T\} \\ \lambda_{\min}\{K_T\} &> \xi_{\bar{m}}\delta_3\lambda_{\max}\{M_T\} + \delta_2\lambda_{\max}\{B_T\} \end{aligned}$$

right-hand side of (163) can be upper bounded as follows

$$\dot{V} \leq -\frac{\min\{\gamma_a, \gamma_b\}}{\bar{\lambda}_2}V + \epsilon \tag{164}$$

where (149) and (151) were utilized, and γ_a, γ_b, $\epsilon \in \mathbb{R}$ denote positive bounding constants.

From (146) - (148), and (151), and that $\hat{F}(t) \in \mathcal{L}_\infty$ (see Appendix D), the expression in (164) can be used with the result from [7] to prove that $\bar{x}(t)$, $\lambda_d(t)$, $\eta_d(t) \in \mathcal{L}_\infty$. Based on (49), and the fact that $\bar{M}^{-1}(x)$, $\hat{F}(t) \in \mathcal{L}_\infty$ then $\dot{\eta}_d(t) \in \mathcal{L}_\infty$. After utilizing the fact that $\eta_d(t)$, $\dot{\eta}_d(t) \in \mathcal{L}_\infty$ along with the Remark 2, then it is clear that $\xi_d(t)$, $\dot{\xi}_d(t)$, $\ddot{\xi}_d(t) \in \mathcal{L}_\infty$. ■

G Existence of the Inverse of $\bar{M}M_T^{-1}$

To show that $\left(\bar{M}M_T^{-1}\right)^{-1}$ term introduced at the right-hand side of (49) exists, from (10) and the fact that M_T is a positive definite, diagonal matrix, then it is clear that

$$\bar{M}M_T^{-1} = S^{-T}\begin{bmatrix} M_1 & 0_{nxn} \\ 0_{nxn} & M_2 \end{bmatrix}S^{-1}M_T^{-1} \tag{165}$$

where S, $M_1(\cdot)$ and $M_2(\cdot)$ were introduced in (8), (1) and (2), respectively. From (165), it is clear that,

$$\left(\bar{M}M_T^{-1}\right)^{-1} = M_T S\begin{bmatrix} M_1^{-1} & 0_{nxn} \\ 0_{nxn} & M_2^{-1} \end{bmatrix}S^T. \tag{166}$$

H Upper Bound Development for MIF Analysis

To simplify the following derivations, (31) can be rewritten as follows

$$\begin{aligned} N &\triangleq N\left(x,\dot{x},\ddot{x},e_1,e_2,r,\dddot{x}_d\right) \\ &= \bar{M}\dddot{x}_d + \dot{\bar{M}}\,\ddot{x} + \dot{\bar{N}} + e_2 \\ &\quad + \bar{M}\left(\alpha_1+\alpha_2\right)r - \bar{M}\left(\alpha_1^2+\alpha_1\alpha_2+\alpha_2^2\right)e_2 \\ &\quad + \bar{M}\alpha_2^3 e_1 + \frac{1}{2}\,\dot{\bar{M}}\,r \end{aligned} \tag{167}$$

where (15) and (16) were both utilized. To facilitate the subsequent analysis, $N\left(x,\dot{x}_d,\ddot{x}_d,0,0,0,\dddot{x}_d\right)$, $N\left(x,\dot{x},\ddot{x}_d,0,0,0,\dddot{x}_d\right)$, $N\left(x,\dot{x},\ddot{x},0,0,0,\dddot{x}_d\right)$, $N\left(x,\dot{x},\ddot{x},e_1,0,0,\dddot{x}_d\right)$, and $N\left(x,\dot{x},\ddot{x},e_1,e_2,0,\dddot{x}_d\right)$ are added and subtracted to the right-hand side of (30) as follows

$$\begin{aligned} &\tilde{N} \\ &= \left[N\left(x,\dot{x}_d,\ddot{x}_d,0,0,0,\dddot{x}_d\right) - N_d\left(x_d,\dot{x}_d,\ddot{x}_d,0,0,0,\dddot{x}_d\right)\right] \\ &\quad + \left[N\left(x,\dot{x},\ddot{x}_d,0,0,0,\dddot{x}_d\right) - N\left(x,\dot{x}_d,\ddot{x}_d,0,0,0,\dddot{x}_d\right)\right] \\ &\quad + \left[N\left(x,\dot{x},\ddot{x},0,0,0,\dddot{x}_d\right) - N\left(x,\dot{x},\ddot{x}_d,0,0,0,\dddot{x}_d\right)\right] \\ &\quad + \left[N\left(x,\dot{x},\ddot{x},e_1,0,0,\dddot{x}_d\right) - N\left(x,\dot{x},\ddot{x},0,0,0,\dddot{x}_d\right)\right] \\ &\quad + \left[N\left(x,\dot{x},\ddot{x},e_1,e_2,0,\dddot{x}_d\right) - N\left(x,\dot{x},\ddot{x},e_1,0,0,\dddot{x}_d\right)\right] \\ &\quad + \left[N\left(x,\dot{x},\ddot{x},e_1,e_2,r,\dddot{x}_d\right) - N\left(x,\dot{x},\ddot{x},e_1,e_2,0,\dddot{x}_d\right)\right]. \end{aligned} \tag{168}$$

After applying the Mean Value Theorem to each bracketed term of (168), the following expression can be obtained

$$\begin{aligned} \tilde{N} &= \\ &\left.\frac{\partial N\left(\sigma_1,\dot{x}_d,\ddot{x}_d,0,0,0,\dddot{x}_d\right)}{\partial\sigma_1}\right|_{\sigma_1=v_1}\left(x-x_d\right) \\ &+ \left.\frac{\partial N\left(x,\sigma_2,\ddot{x}_d,0,0,0,\dddot{x}_d\right)}{\partial\sigma_2}\right|_{\sigma_2=v_2}\left(\dot{x}-\dot{x}_d\right) \\ &+ \left.\frac{\partial N\left(x,\dot{x},\sigma_3,0,0,0,\dddot{x}_d\right)}{\partial\sigma_3}\right|_{\sigma_3=v_3}\left(\ddot{x}-\ddot{x}_d\right) \\ &+ \left.\frac{\partial N\left(x,\dot{x},\ddot{x},\sigma_4,0,0,\dddot{x}_d\right)}{\partial\sigma_4}\right|_{\sigma_4=v_4}\left(e_1-0\right) \\ &+ \left.\frac{\partial N\left(x,\dot{x},\ddot{x},e_1,\sigma_5,0,\dddot{x}_d\right)}{\partial\sigma_5}\right|_{\sigma_5=v_5}\left(e_2-0\right) \\ &+ \left.\frac{\partial N\left(x,\dot{x},\ddot{x},e_1,e_2,\sigma_6,\dddot{x}_d\right)}{\partial\sigma_6}\right|_{\sigma_6=v_6}\left(r-0\right) \end{aligned} \tag{169}$$

where $v_1 \in (x_d, x)$, $v_2 \in (\dot{x}_d, \dot{x})$, $v_3 \in (\ddot{x}_d, \ddot{x})$, $v_4 \in (0, e_1)$, $v_5 \in (0, e_2)$, and $v_6 \in (0, r)$. The right-hand side of (169) can be upper bounded as follows

$$\begin{aligned} \left\|\tilde{N}\right\| &\leq \\ &\left\|\left.\frac{\partial N\left(\sigma_1,\dot{x}_d,\ddot{x}_d,0,0,0,\dddot{x}_d\right)}{\partial\sigma_1}\right|_{\sigma_1=v_1}\right\|\left\|e_1\right\| \\ &+ \left\|\left.\frac{\partial N\left(x,\sigma_2,\ddot{x}_d,0,0,0,\dddot{x}_d\right)}{\partial\sigma_2}\right|_{\sigma_2=v_2}\right\|\left\|\dot{e}_1\right\| \\ &+ \left\|\left.\frac{\partial N\left(x,\dot{x},\sigma_3,0,0,0,\dddot{x}_d\right)}{\partial\sigma_3}\right|_{\sigma_3=v_3}\right\|\left\|\ddot{e}_1\right\| \\ &+ \left\|\left.\frac{\partial N\left(x,\dot{x},\ddot{x},\sigma_4,0,0,\dddot{x}_d\right)}{\partial\sigma_4}\right|_{\sigma_4=v_4}\right\|\left\|e_1\right\| \\ &+ \left\|\left.\frac{\partial N\left(x,\dot{x},\ddot{x},e_1,\sigma_5,0,\dddot{x}_d\right)}{\partial\sigma_5}\right|_{\sigma_5=v_5}\right\|\left\|e_2\right\| \\ &+ \left\|\left.\frac{\partial N\left(x,\dot{x},\ddot{x},e_1,e_2,\sigma_6,\dddot{x}_d\right)}{\partial\sigma_6}\right|_{\sigma_6=v_6}\right\|\left\|r\right\|. \end{aligned} \tag{170}$$

The partial derivatives in (169) can be calculated by using (167) as follows

$$\begin{aligned} \frac{\partial N\left(\sigma_1,\dot{x}_d,\ddot{x}_d,0,0,0,\dddot{x}_d\right)}{\partial\sigma_1} &= \frac{\partial\bar{M}\left(\sigma_1\right)}{\partial\sigma_1}\dddot{x}_d \\ &\quad + \frac{\partial\,\dot{\bar{M}}\left(\sigma_1,\dot{x}_d\right)}{\partial\sigma_1}\ddot{x}_d \\ &\quad + \frac{\partial\,\dot{\bar{N}}\left(\sigma_1,\dot{x}_d,\ddot{x}_d\right)}{\partial\sigma_1} \end{aligned} \tag{171}$$

$$\begin{aligned} \frac{\partial N\left(x,\sigma_2,\ddot{x}_d,0,0,0,\dddot{x}_d\right)}{\partial\sigma_2} &= \frac{\partial\,\dot{\bar{M}}\left(x,\sigma_2\right)}{\partial\sigma_2}\ddot{x}_d \\ &\quad + \frac{\partial\,\dot{\bar{N}}\left(x,\sigma_2,\ddot{x}_d\right)}{\partial\sigma_2} \end{aligned} \tag{172}$$

$$\begin{aligned} \frac{\partial N\left(x,\dot{x},\sigma_3,0,0,0,\dddot{x}_d\right)}{\partial\sigma_3} &= \dot{\bar{M}}\left(x,\dot{x}\right) \\ &\quad + \frac{\partial\,\dot{\bar{N}}\left(x,\dot{x},\sigma_3\right)}{\partial\sigma_3} \end{aligned} \tag{173}$$

$$\frac{\partial N\left(x,\dot{x},\ddot{x},\sigma_4,0,0,\dddot{x}_d\right)}{\partial\sigma_4} = \alpha_2^3\bar{M}\left(x\right) \tag{174}$$

$$\begin{aligned} \frac{\partial N\left(x,\dot{x},\ddot{x},e_1,\sigma_5,0,\dddot{x}_d\right)}{\partial\sigma_5} &= I_{2n} \\ &\quad - \left(\alpha_1^2+\alpha_1\alpha_2+\alpha_2^2\right)\bar{M}\left(x\right) \end{aligned} \tag{175}$$

$$\begin{aligned} \frac{\partial N\left(x,\dot{x},\ddot{x},e_1,e_2,\sigma_6,\dddot{x}_d\right)}{\partial\sigma_6} &= \left(\alpha_1+\alpha_2\right)\bar{M}\left(x\right) \\ &\quad + \frac{1}{2}\,\dot{\bar{M}}\left(x,\dot{x}\right) \end{aligned} \tag{176}$$

where $I_{2n} \in \mathbb{R}^{2n\times 2n}$ denotes the identity matrix. By defining

$$\begin{aligned} v_1 &\triangleq x - \tau_1\left(x-x_d\right) & v_2 &\triangleq \dot{x} - \tau_2\left(\dot{x}-\dot{x}_d\right) \\ v_3 &\triangleq \ddot{x} - \tau_3\left(\ddot{x}-\ddot{x}_d\right) & v_4 &\triangleq e_1 - \tau_4\left(e_1-0\right) \\ v_5 &\triangleq e_2 - \tau_5\left(e_2-0\right) & v_6 &\triangleq r - \tau_6\left(r-0\right) \end{aligned}$$

where $\tau_i \in (0,1)\ \forall i = 1,2,...,6$, and if the assumptions stated for the system model and the desired trajectory are met, then upper bounds for the right-hand sides of (171)-(176) can be rewritten as follows

$$\left\| \frac{\partial N\left(\sigma_1, \dot{x}_d, \ddot{x}_d, 0, 0, 0, \dddot{x}_d\right)}{\partial \sigma_1}\bigg|_{\sigma_1 = v_1} \right\| \leqslant \rho_1\left(x, \dot{x}, \ddot{x}\right) \quad (177)$$

$$\left\| \frac{\partial N\left(x, \sigma_2, \ddot{x}_d, 0, 0, 0, \dddot{x}_d\right)}{\partial \sigma_2}\bigg|_{\sigma_2 = v_2} \right\| \leqslant \rho_2\left(x, \dot{x}, \ddot{x}\right) \quad (178)$$

$$\left\| \frac{\partial N\left(x, \dot{x}, \sigma_3, 0, 0, 0, \dddot{x}_d\right)}{\partial \sigma_3}\bigg|_{\sigma_3 = v_3} \right\| \leqslant \rho_3\left(x, \dot{x}\right) \quad (179)$$

$$\left\| \frac{\partial N\left(x, \dot{x}, \ddot{x}, \sigma_4, 0, 0, \dddot{x}_d\right)}{\partial \sigma_4}\bigg|_{\sigma_4 = v_4} \right\| \leqslant \rho_4\left(x\right) \quad (180)$$

$$\left\| \frac{\partial N\left(x, \dot{x}, \ddot{x}, e_1, \sigma_5, 0, \dddot{x}_d\right)}{\partial \sigma_5}\bigg|_{\sigma_5 = v_5} \right\| \leqslant \rho_5\left(x\right) \quad (181)$$

$$\left\| \frac{\partial N\left(x, \dot{x}, \ddot{x}, e_1, e_2, \sigma_6, \dddot{x}_d\right)}{\partial \sigma_6}\bigg|_{\sigma_6 = v6} \right\| \leqslant \rho_6\left(x, \dot{x}\right) \quad (182)$$

where $\rho_i(\cdot)\ \forall i = 1,2,...,6$, are positive nondecreasing functions of $x(t)$, $\dot{x}(t)$, and $\ddot{x}(t)$. After substituting (177)-(182) into (170), $\tilde{N}(\cdot)$ can be rewritten as

$$\begin{aligned} \tilde{N} \leq\ & \left[\rho_1\left(\|e_1\|, \|e_2\|, \|r\|\right) + \rho_4\left(\|e_1\|\right)\right]\|e_1\| \quad (183) \\ & + \rho_2\left(\|e_1\|, \|e_2\|, \|r\|\right)\|\dot{e}_1\| \\ & + \rho_3\left(\|e_1\|, \|e_2\|\right)\|\ddot{e}_1\| \\ & + \rho_5\left(\|e_1\|\right)\|e_2\| \\ & + \rho_6\left(\|e_1\|, \|e_2\|\right)\|r\| \end{aligned}$$

where (15) and (16) were utilized. The expressions in (15), (16) and (97) can be used to rewrite the upper bound for the right-hand side of (183) as in (101).

I MIF Controller Simulation Results

A numerical simulation was performed to demonstrate the performance of the MIF controller given in (26) and (34). A 2-link, revolute robot dynamic model was utilized for both the master and slave systems [34] where $M_i(\cdot)$ and $N_i(\cdot)$ are defined as follows

$$\begin{aligned} M_i &= \begin{bmatrix} 3.12 + 2\sin\left(q_{i2}\right) & 0.75 + \sin\left(q_{i2}\right) \\ 0.75 + \sin\left(q_{i2}\right) & 0.75 \end{bmatrix} \quad (184) \\ N_i &= \begin{bmatrix} \sin\left(q_{i2}\right)\dot{q}_{i2} & \sin\left(q_{i2}\right)\left(\dot{q}_{i1} + \dot{q}_{i2}\right) \\ -\sin\left(q_{i2}\right)\dot{q}_{i1} & 0 \end{bmatrix} \begin{bmatrix} \dot{q}_{i1} \\ \dot{q}_{i2} \end{bmatrix} \end{aligned}$$

where $i = 1$ denotes the master system and $i = 2$ denotes the slave system. By utilizing the forward kinematics [34], the task-space dynamic model is used in the simulation. The task-space user and environmental input forces were set equal to the following time-varying signals

$$F_H = \begin{bmatrix} -\sin(t) \\ -\cos(t) \end{bmatrix} \quad F_E = \begin{bmatrix} -0.18\dot{x}_{s1} - 0.3x_{s1} \\ -0.18\dot{x}_{s2} - 0.3x_{s2} \end{bmatrix}. \quad (185)$$

The target system, described by (20) and (21), is defined as follows

$$\dot{\xi}_p = \gamma\varphi\left(\xi_p\right) + \eta_d \quad (186)$$

$$M_T \begin{bmatrix} \dot{\eta}_{dx} \\ \dot{\eta}_{dy} \end{bmatrix} = F_H + F_E \quad (187)$$

where $M_T = I_2$ where $I_2 \in \mathbb{R}^{2\times 2}$ denotes the identity matrix and the terms B_T, and K_T are selected to be zero. The following planar task-space velocity field was utilized [2]

$$\varphi\left(\xi_p\right) \triangleq -2K\left(\xi_p\right) f\left(\xi_p\right)\xi_p + 2c\left(\xi_p\right)\begin{bmatrix} -\xi_{py} \\ \xi_{px} \end{bmatrix} \quad (188)$$

where $\xi_p = \begin{bmatrix} \xi_{px} & \xi_{py} \end{bmatrix}^T$ is the desired end-effector position, and $f(\cdot)$, $K(\cdot)$, $c(\cdot) \in \mathbb{R}$ are defined as follows

$$\begin{aligned} f\left(\xi_p\right) &\triangleq \xi_{px}^2 + \xi_{py}^2 - r_o^2 \quad (189) \\ K\left(\xi_p\right) &\triangleq k_o\left(\sqrt{f^2\left(\xi_p\right)}\left\|\frac{\partial f\left(\xi_p\right)}{\partial \xi_p}\right\| + \epsilon\right)^{-1} \\ c\left(\xi_p\right) &\triangleq \frac{c_o \exp\left(-\mu\sqrt{f^2\left(\xi_p\right)}\right)}{\left\|\frac{\partial f(\xi_p)}{\partial \xi_p}\right\|}. \end{aligned}$$

In (189), $r_o = 1$ [m] denotes the circle radius, $k_o = 3\left[\mathrm{ms}^{-1}\right]$, $\epsilon = 0.005\left[\mathrm{m}^3\right]$, $c_o = 0.25\left[\mathrm{ms}^{-1}\right]$, and $\mu = 20\left[\mathrm{m}^{-1}\right]$ were selected for the simulation. For the simulation, the user assist mechanism is enabled, hence, $\gamma = 1$. The controller gains are selected as $k_s = 100$, $\beta_1 + \beta_2 = 100$, and $\alpha_1 = \alpha_2 = 2$.

In Figure 1, the desired end-effector position $\xi_p(t)$ is presented when the user assist mechanism is disabled (i.e., $\gamma = 0$) where the environmental force vector $F_E(t)$ is assumed to be zero. From Figure 1, it is clear that the user can create a circular desired trajectory. For the remaining simulation runs, environmental force vector $F_E(t)$ is set to be a spring-like input force vector, as defined in (185). The desired end-effector position $\xi_p(t)$, when the user assist mechanism is disabled (i.e., $\gamma = 0$) and when the user assist mechanism is enabled (i.e., $\gamma = 1$) are presented Figure 2. From Figure 2, it is clear that the user can not create a circular desired trajectory in the presence of the environmental input force. When the user assist

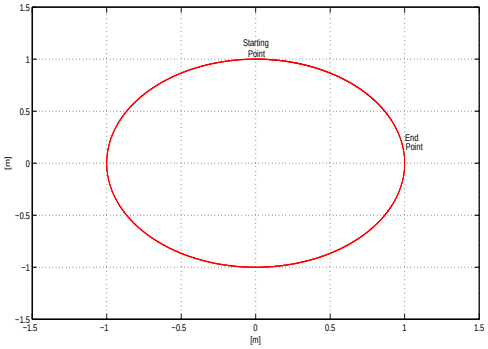

Figure 1: The desired end-effector position $\xi_p(t)$ when the user assist mechanism is disabled (i.e., $\gamma = 0$) and the environmental input force $F_E(t)$ is assumed to be zero

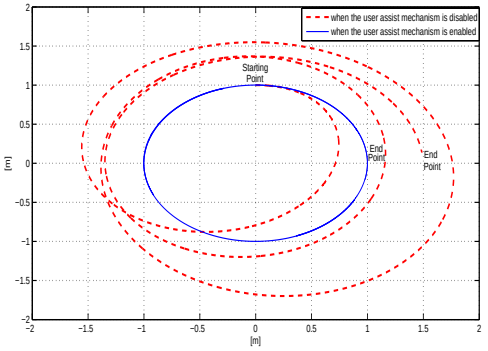

Figure 2: Desired End-Effector Position $\xi_p(t)$

mechanism is enabled (i.e., $\gamma = 1$), then the user can create a circular desired trajectory even in the presence of environmental force. The end-effector positions for the master and the slave systems are given in Figures 3 and 4, respectively. The master system tracking error $e_{11}(t)$ and coordination error $e_{12}(t)$ are presented in Figures 5 and 6, respectively. From Figures 5 and 6, it is clear that tracking and coordination control objectives defined in (4) and (5), are met. The control inputs for the master system $T_1(t)$ and the slave system $T_2(t)$ are provided in Figures 7 and 8, respectively.

J UMIF Controller Simulation Results

A numerical simulation was performed for the UMIF controller given in (54) and (57). The 2-link, revolute robot dynamic model introduced in (184) was utilized for both the master and slave systems. By utilizing the exact model knowledge of the simulated system, $\bar{F}(t)$ in-

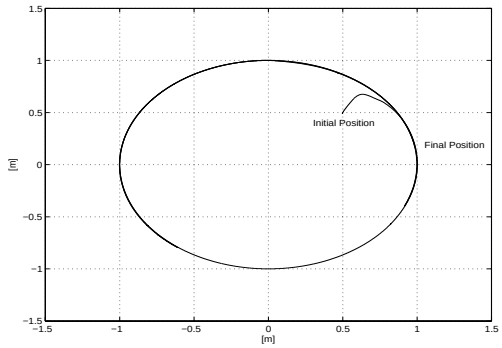

Figure 3: Master System End-Effector Position $x_m(t)$ when the user assist mechanism is enabled (i.e., $\gamma = 1$)

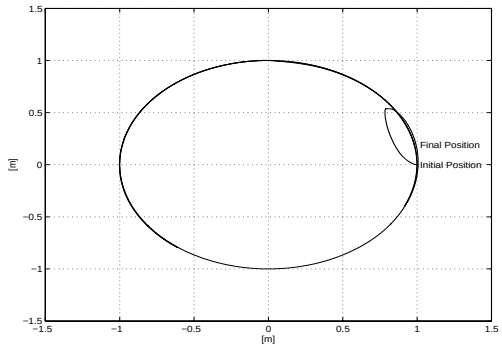

Figure 4: Slave System End-Effector Position $x_s(t)$ when the user assist mechanism is enabled (i.e., $\gamma = 1$)

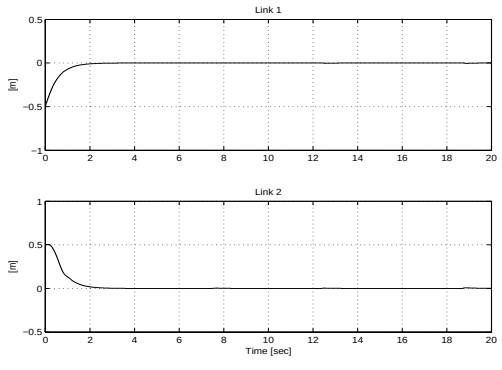

Figure 5: Master System Tracking Error $e_{11}(t)$ when the user assist mechanism is enabled (i.e., $\gamma = 1$)

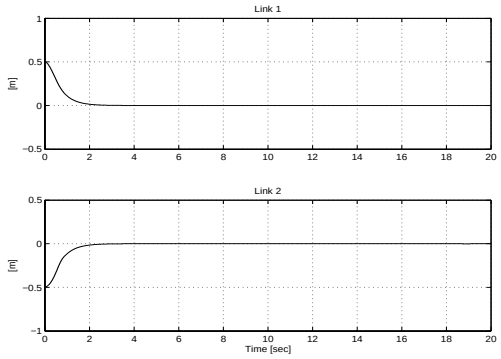

Figure 6: Coordination Error $e_{12}(t)$ when the user assist mechanism is enabled (i.e., $\gamma = 1$)

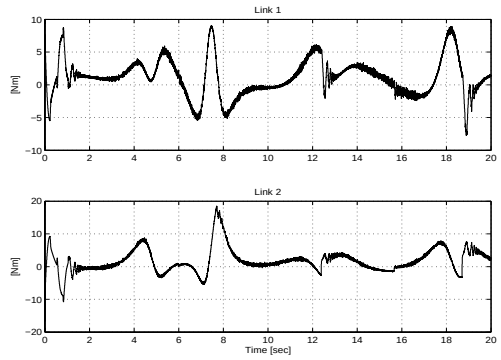

Figure 7: Control Input for Master System $T_1(t)$ when the user assist mechanism is enabled (i.e., $\gamma = 1$)

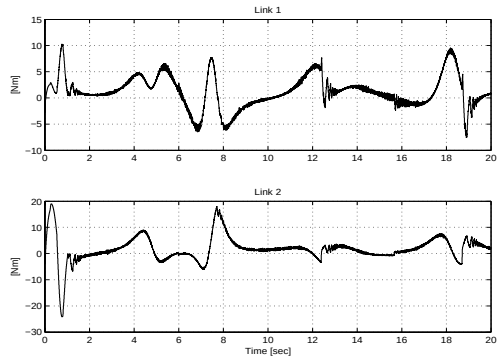

Figure 8: Control Input for Slave System $T_2(t)$ when the user assist mechanism is enabled (i.e., $\gamma = 1$)

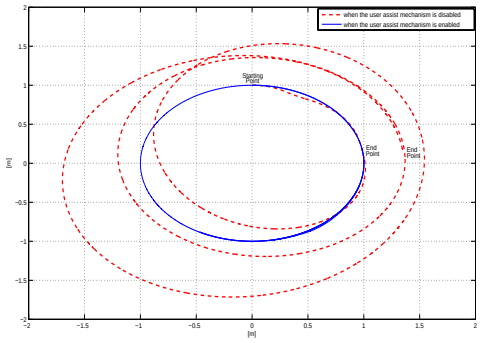

Figure 9: Desired End-Effector Position $\xi_{d1p}(t)$

troduced in (13) is defined as follows

$$\bar{F} = \bar{M} M_T^{-1} \begin{bmatrix} F_H + F_E \\ -F_E \end{bmatrix} \tag{190}$$

where $F_H(t)$ and $F_E(t)$ were defined in (185). The planar task-space velocity field defined in (188) was utilized with the same parameters. The constants for the target system, described by (49), are set to $M_T = I_4$, where $I_4 \in \mathbb{R}^{4\times 4}$ denotes the identity matrix and the terms B_T and K_T are selected to be zero. The controller gains are selected as $k_s = 100$, $\beta_1 + \beta_2 = 100$, and $\alpha = 1$.

The desired end-effector position $\xi_{1p}(t)$, when the user assist mechanism is disabled (i.e., $\gamma = 0$) and when the user assist mechanism is enabled (i.e., $\gamma = 1$) are presented Figure 9. From Figure 9, it is clear that the proposed user assist mechanism provides a major improvement to the desired end-effector position. The end-effector positions for the master and the slave systems are given in Figures 10 and 11, respectively. The master system tracking error $e_{11}(t)$ and the coordination error $e_{12}(t)$ are presented in Figures 12 and 13, respectively. From Figures 12 and 13, it is clear that tracking and coordination control objectives defined in (40) and (41), are met. The control inputs for the master system $T_1(t)$ and the slave system $T_2(t)$ are provided in Figures 14 and 15, respectively. The output of the nonlinear force observer $\hat{F}(t)$ is presented in Figure 16.

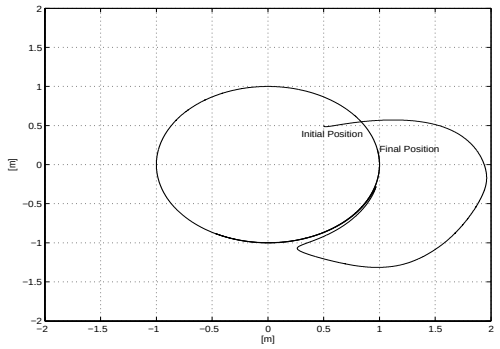

Figure 10: Master System End-Effector Position $x_m(t)$ when the user assist mechanism is enabled (i.e., $\gamma = 1$)

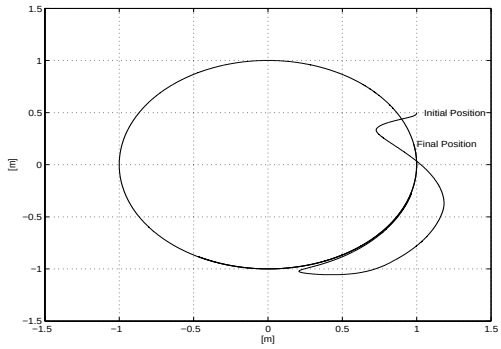

Figure 11: Slave System End-Effector Position $x_s(t)$ when the user assist mechanism is enabled (i.e., $\gamma = 1$)

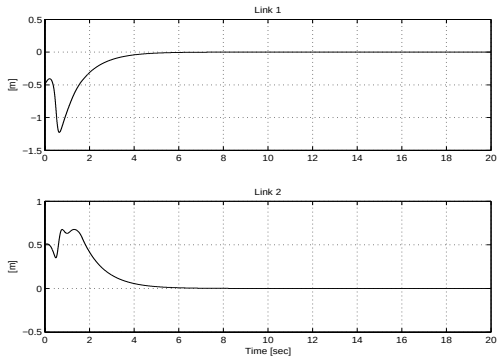

Figure 12: Master System Tracking Error $e_{11}(t)$ when the user assist mechanism is enabled (i.e., $\gamma = 1$)

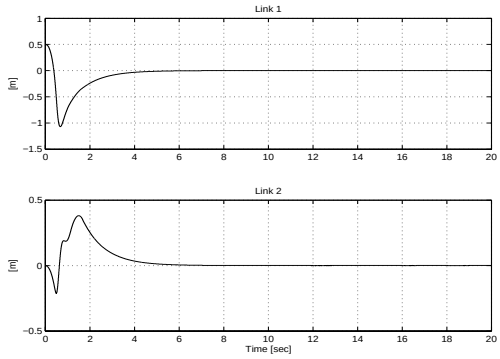

Figure 13: Coordination Error $e_{12}(t)$ when the user assist mechanism is enabled (i.e., $\gamma = 1$)

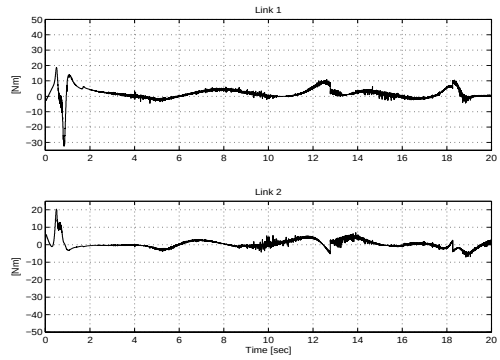

Figure 14: Torque Input for Master System $T_1(t)$ when the user assist mechanism is enabled (i.e., $\gamma = 1$)

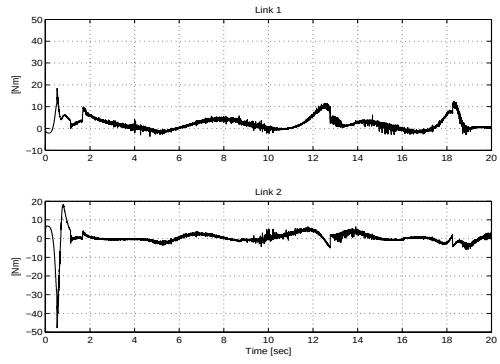

Figure 15: Torque Input for Slave System $T_2(t)$ when the user assist mechanism is enabled (i.e., $\gamma = 1$)

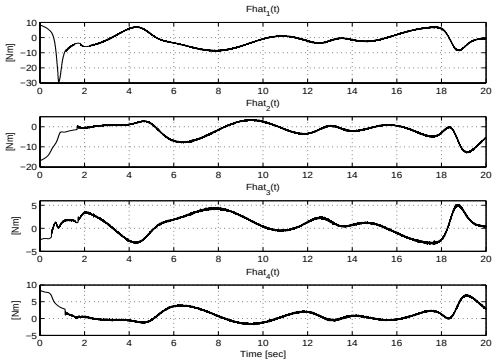

Figure 16: The Output of the Nonlinear Force Observer $\hat{F}(t)$ when the user assist mechanism is enabled (i.e., $\gamma = 1$)